
VOC measurements by PTR-ToF-MS at the Birkenes Observatory

A data summary report

Stephan Langebner, Tomáš Mikoviny, Markus Müller and Armin
Wisthaler



Scientific report

Preface

This document is a Data Summary Report presenting background information, analytical methods, and analytical results of a volatile organic compound (VOC) study conducted at the Birkenes Observatory in Southern Norway.

The study was carried out in joint work by NILU - Norwegian Institute of Air Research and the University of Innsbruck (UIBK) in Austria. Part of the experimental work and the entire data analysis was carried out by Stephan Langebner (UIBK) during his research stay at NILU. Tomáš Mikoviny (UIBK) provided experimental support. Markus Müller (UIBK) contributed to data analysis and data quality control. Armin Wisthaler (NILU, UIBK) led the project and supervised the work.

The work was partly supported by EMEP, the EU FP7 Project ACTRIS and the Research Council of Norway under the Strategisk instituttsatsing (SIS) program.

We thank Terje Krognnes, Olav Lien, Chris Lunder, Norbert Schmidbauer and Harald Willoch for logistical support, Sverre Solberg for helpful comments and Wenche Aas for initiating the measurements.

Contents

	Page
Preface	1
Summary	5
1 Introduction	7
2 Methodology	9
2.1 Measurement site.....	9
2.2 Instrumentation (PTR-ToF-MS)	10
2.3 Data-quality control and reduction, data archival	13
3 Results	14
3.1 Full mass spectrum analysis.....	14
3.2 PTR-MS standard data product.....	15
3.2.1 m/z 33.033 (methanol)	17
3.2.2 m/z 42.035 (acetonitrile)	18
3.2.3 m/z 45.032 (acetaldehyde)	19
3.2.4 m/z 59.048 (acetone)	20
3.2.5 m/z 63.028 (dimethyl sulphide).....	21
3.2.6 m/z 69.070 (isoprene).....	22
3.2.7 m/z 71.049 (sum of methylvinylketone and methacrolein).....	23
3.2.8 m/z 73.065 (methylethylketone).....	24
3.2.9 m/z 79.054 (benzene)	25
3.2.10 m/z 93.069 (toluene).....	26
3.2.11 m/z 107.085 (sum of C ₈ -alkylbenzene isomers).....	27
3.2.12 m/z 121.103 (sum of C ₉ -alkylbenzene isomers).....	28
3.2.13 m/z 137.133 (sum of monoterpene isomers)	29
3.3 PTR-MS exploratory data product	30
3.3.1 m/z 47.012 (formic acid)	31
3.3.2 m/z 61.028 (acetic acid)	32
3.3.3 m/z 87.080 (unidentified)	33
3.3.4 m/z 89.060 (unidentified)	34
3.3.5 m/z 101.098 (unidentified)	35
3.3.6 m/z 151.110 (pinonaldehyde).....	36
3.4 A preliminary analysis of the monoterpenes and isoprene data.....	37
4 References	40
Appendix A Discussion on local contamination	43

Summary

A high resolution proton-transfer-reaction time-of-flight mass spectrometer (PTR-ToF-MS) was used for on-line and real-time measurements of volatile organic compounds (VOCs) at the Birkenes Observatory in Southern Norway. Measurements were carried out during late spring and summer 2012 and in January and early February 2013. Here we present the obtained PTR-MS standard data product which includes volume mixing ratios of methanol, acetonitrile, acetaldehyde, acetone, dimethyl sulphide, isoprene, methacrolein plus methylvinylketone, methylethylketone, benzene, toluene, C₈-alkylbenzenes, C₉-alkylbenzenes and the sum of the monoterpene isomers. Exploratory data of formic acid, acetic acid, pinonaldehyde and three unidentified signals (m/z 87.080, m/z 89.060 and m/z 101.098) are also shown. PTR-ToF-MS mass spectra were dominated by oxygenated VOCs both in summer and in winter. Pure hydrocarbons were mostly aromatic hydrocarbons (benzene, toluene, C₈-alkylbenzenes) in winter and biogenic hydrocarbons (monoterpenes and isoprene) in summer. The summertime data confirm that the Birkenes Observatory is an interesting site in the boreo-nemoral vegetation zone where it is possible to observe both monoterpene and isoprene emissions and their photochemical processing in the atmosphere.

VOC measurements by PTR-ToF-MS at the Birkenes Observatory

1 Introduction

The interaction between the atmosphere and the biosphere is an important research focus in Earth science. Key study areas include the exchange of greenhouse gases but also of more reactive gases such as reduced and oxidized nitrogen compounds (NH_3 , NO_x , NO_y) and volatile organic compounds (VOCs). Emissions of biogenic volatile organic compounds (BVOCs) from forest ecosystems affect both local and regional air quality through photochemical reactions with the hydroxyl and nitrate radicals and ozone, and through secondary aerosol formation. The latter may also have important implications in the context of global climate change.

Long-range transport of reactive oxidized nitrogen species and of anthropogenic volatile organic compounds (AVOCs) may lead to photochemical air pollution (e.g. ozone formation) over remote forested areas with potential adverse effects on vegetation.

Over the past decades, VOC measurements have been performed in various forest ecosystems with a focus on tropical forests in the Southern Hemisphere and on boreal and nemoral forests in the Northern Hemisphere.

A relatively small but interesting vegetation zone is the so-called boreo-nemoral zone which consists of mixed coniferous and broad-leaved forests. In Scandinavia, this zone includes parts of South and Southwest Norway, the south of Sweden and the very southern part of Finland (Figure 1).

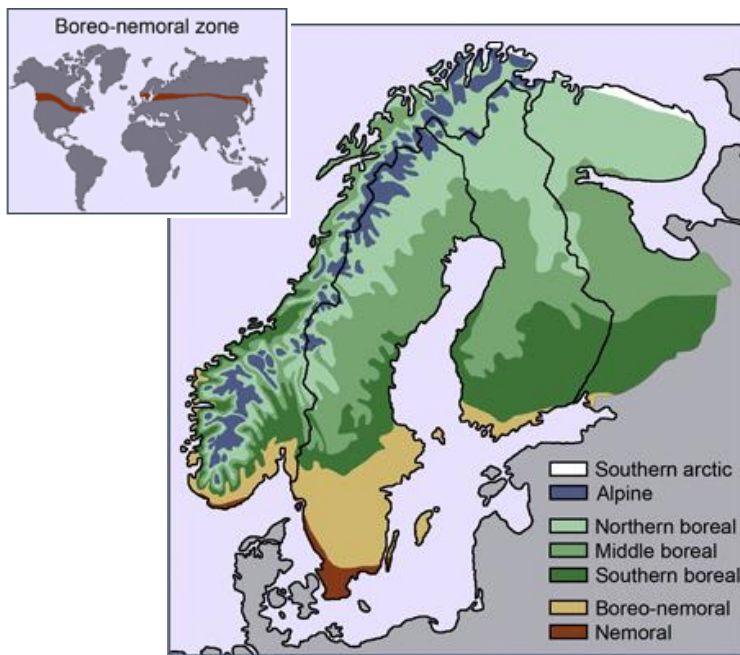


Figure 1: Geographical maps showing the extension of the boreo-nemoral forest zone (globally and in Northern Europe) (figure courtesy: B. Elmhagen).

From a biosphere-atmosphere interaction point of view, the boreo-nemoral zone is interesting under various aspects. It represents the transition zone where the vegetation changes from predominant isoprene emitters to predominant monoterpene emitters, with both reactive species being present in the atmosphere at significant levels. In addition, the boreo-nemoral region is situated close to major source regions of anthropogenic air pollutants in North America, Europe and Asia and frequent transport of man-made pollutants has potential implications for the boreo-nemoral forest ecosystem and atmospheric chemistry in the region. The mix of isoprene and monoterpenes emissions in combination with advected anthropogenic air pollutants represents a particular challenge and valuable test ground for atmospheric chemistry transport models. Ultimately, the boreo-nemoral forest region may grow in extension shifting northward due to climate change. The specific biosphere-atmosphere interactions observed in this region may thus become more important in the future.

Based on these motivations, we have conducted a summer- and wintertime VOC screening study in Southern Norway using the most state-of-the-art on-line and real-time instrumentation that is currently available.

2 Methodology

2.1 Measurement site

NILU - Norwegian Institute of Air Research (NILU - Norsk institutt for luftforskning) operates a regional atmospheric background observatory in the Birkenes municipality in Southern Norway (Figure 2).



Figure 2: Geographic location of the Birkenes Observatory (taken from Google Earth).

The first measurement station was built in 1971. It is located at 58°23'0"N, 8°15'0" E at an altitude of 190 m asl. We herein refer to this site as the Birkenes I station. A new observatory was established in 2009. The new station (herein referred to as Birkenes II) is positioned in close proximity to the old station at 58°23'18"N, 8°15'7"E, at an altitude of 219 m asl on the hill above the old station.

Local human influence is limited to low intensity agricultural activities on isolated farms (Figure 3) and very low traffic activities (< 5 vehicles per day). The closest minor settlement is Birkeland (6.5 km S, 2500 inhabitants). Major settlements (> 10.000 inhabitants) in 20 to 35 km distance are Arendal (ENE), Grimstad (E), Kristiansand (SSW) and Venneå (SW).

The terrain is hilly and densely forested (Figure 3). The land use within 1 km of the site is characterized by 65 % forest; the remaining 35 % is attributed to meadow (10 %), low intensity agricultural areas (10 %), and freshwater lakes (15 %) (Yttri et al., 2011).

The Birkenes observatory is situated in the boreo-nemoral vegetation zone dominated by coniferous trees, Norway spruce (*Picea abies*) and Scots pine (*Pinus sylvestris*). A monitored forest area in the immediate vicinity of the

measurement site is dominated by naturally grown Norway Spruce (~ 130 years in age) (Timmermann et al., 2013). The greater area includes patches of mixed deciduous coniferous forests and pure deciduous forest (Figure 4). The dominating deciduous tree species in the region are sessile oak (*Quercus petraea* Liebl.), aspen (*Populus tremula* L.), and birch (*Betula* spp.).

Due to the close proximity (tens of km) to the Southern coast of Norway, the Birkenes site also experiences a strong marine influence (Wright, 2008; Yttri et al., 2011).

Long-range transport of air pollutants to the Birkenes Observatory has been addressed in a series of previous studies (e.g. Amundsen et al., 1992; Tørseth et al., 2001; Eckhardt et al., 2009; Tørseth et al., 2012).

2.2 Instrumentation (PTR-ToF-MS)

A PTR-TOF 8000 (Ionicon Analytik GmbH, Innsbruck, Austria) was used for on-line and real-time measurements of VOCs at the Birkenes Observatory. PTR-ToF-MS measurements were carried out from April 28, 2012 to August 30, 2012 (summer campaign 2012) and from January 12, 2013 to February 8, 2013 (winter campaign 2013).

The measurement principle and the PTR-TOF 8000 instrument itself have been described in great detail elsewhere (Jordan et al., 2009) and thus only the essentials are described here.

Ambient air is drawn into a low-pressure reactor where organic molecules react with hydronium ions (H_3O^+) generated in an external glow discharge ion source. A voltage across the reactor, precisely termed drift tube, generates an electric field which prevents hydration of ions. Non-dissociative proton transfer reactions result in the formation of protonated organic analyte molecules that can be subjected to mass spectrometric analysis. Highly mass resolved analysis in the PTR-TOF 8000 instrument identifies the sum formula of the analyte ions.

During the measurement campaigns described herein, the PTR-TOF 8000 was operated in its routine mode of operation. The drift tube pressure was 2.25 mbar, the drift tube temperature was 60 °C and the drift tube voltage was 550 V. Mass spectra were recorded in the mass-to-charge (m/z) 0-310 range using a one minute signal integration.

For data analysis, the “PTR-TOF Data Analyzer” software in versions 2.45 to 3.52 was used (Müller et al., 2013).

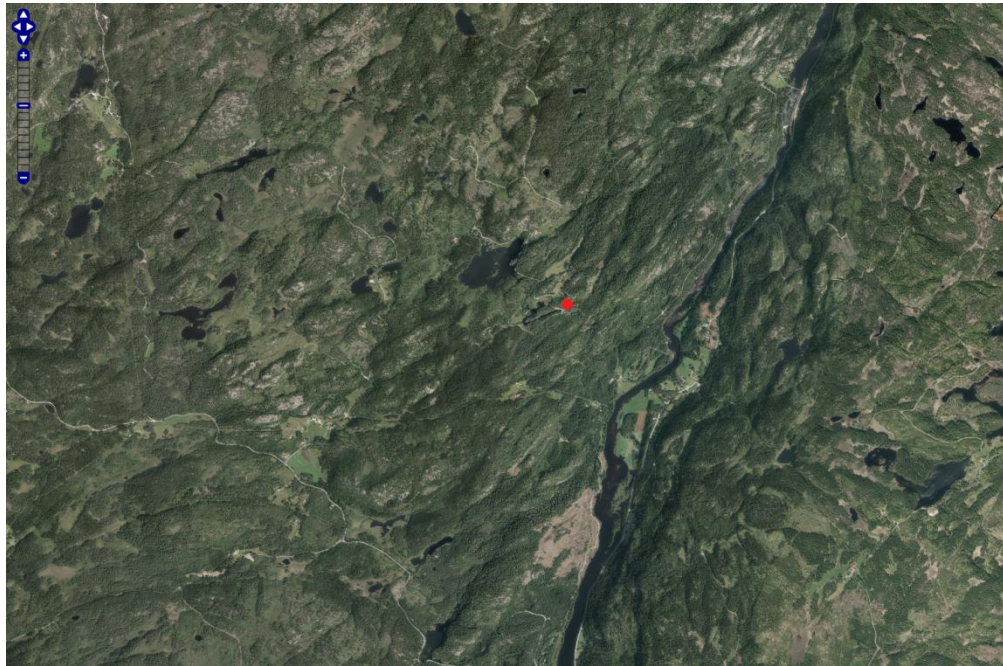


Figure 3: Orthophoto (1:20000; 8 x 5 km) of the area surrounding the sampling site. The position of the Birkenes Observatory is marked by a red dot. (source: Norsk institutt for skog og landskap via <http://kilden.skogoglandskap.no/>).

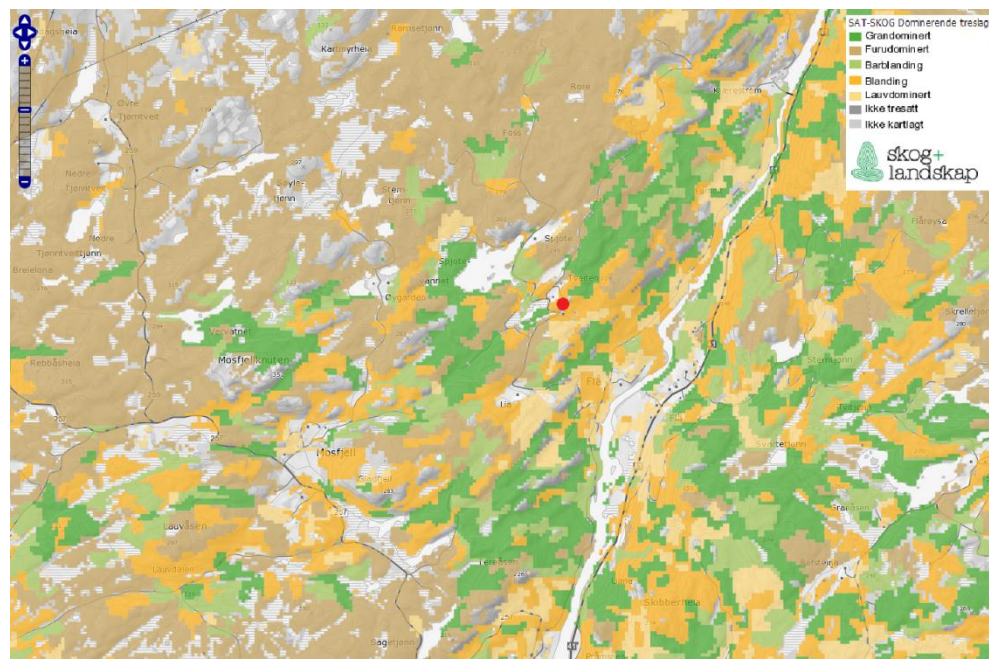


Figure 4: Forest map (1:20000; 8 x 5 km) of the area surrounding the sampling site. The position of the Birkenes Observatory is marked by a red dot. Dark green: spruce-dominated; light green: mixed spruce and pine (> 75 %); light brown: pine-dominated; mustard (dark) yellow: mixed; light yellow: deciduous; grey: not forested or no info (source: SAT-SKOG, Norsk institutt for skog og landskap via <http://kilden.skogoglandskap.no/>).



Figure 5: Photograph of the sampling inlet used for the measurements at the Birkenes Observatory.

A 1/4" (6.35 mm) Teflon® PFA tube was used to draw outside air into the measurement container at a controlled flow of 3 standard liters per minute (slpm). The tube was temperature stabilized to 60 °C and capped with a Teflon® PFA filter holder including a 0.2 µm pore size Teflon® PFA particulate filter (Entegris, Billerica, MA, USA).

The PTR-ToF-MS instrument sub-sampled a small portion (~ 100 standard cubic centimeters per minute, sccm) of the main inlet flow through a heated (60 °C) 1/8" (3.175 mm) Teflon® PFA tube.

For external mass axis calibration, a small flow (~ 2 sccm) of ultra-pure synthetic air containing ppm levels of 3-fluoro-o-xylene ($[M+H]^+$ detected at m/z 125.076) and 1,4-di(trifluoromethyl)benzene ($[M-HF]^+$ detected at m/z 195.022), respectively, was continuously added to the PTR-ToF-MS sampling flow from a pressurized canister.

For zeroing, the PTR-ToF-MS inlet was overflowed with VOC-free air generated from compressed and catalytically cleaned ambient air. A commercial noble metal catalyst module (Parker Hannifin Corp., Haverhill, MA, USA) operated at 350 °C was used for the generation of VOC-free air.

For calibration, VOC-free air was spiked with a certified VOC standard gas (Apel-Riemer Environmental Inc., Broomfield, CO, USA) to generate accurate mixing ratios of selected organic trace gases at ppbv-levels. The VOC standard gas contained 1 ppmv of methanol, acetonitrile, acetaldehyde, acrolein, acetone, isoprene, MEK, benzene, toluene, hexanal, p-xylene, 1,3,5-trimethylbenzene, 1,2,4,5-tetramethylbenzene, and α -pinene, respectively. The nominal accuracy of the VOC calibration mix is $\pm 5\%$; for oxygenated species we put a more conservative $\pm 15\%$ estimate on the accuracy of the measurements.

The zeroing and calibration procedure was fully automated. Teflon® solenoid valves (M Series, Teqcom Industries Inc., Santa Ana, USA) were activated via the PTR-Manager software (Icon Analytik GmbH, Innsbruck, Austria) to divert the zero air flow and/or the calibration gas flow into the PTR-ToF-MS instrument. Zeroing was performed three times a week for 30 min. A single-point calibration was carried out once a week, multi-point calibrations were performed before and after the measurement campaigns.

2.3 Data-quality control and reduction, data archival

Data obtained during periods with instrumental deficiencies (ion source instabilities and software acquisition problems) were removed.

For instrumental background correction, the signals obtained during the zeroing periods were linearly interpolated.

For calibration, the instrumental response factors obtained during weekly calibration exercises were also linearly interpolated.

Data affected by local contamination arising from human activities at the measurement station (as noted in the station logbook) were also removed from the dataset. It is noted here that the m/z 57.070 local contamination tracer (i.e. $C_4H_9^+$ ions formed upon fragmentation of long-chain hydrocarbons generated from local combustion engine emissions) showed occasional increases also during periods not noted in the station logbook. A more detailed discussion is given in Appendix A. The conclusions drawn in this work are, however, not affected by a potential bias due to local contamination.

Data were grouped into a PTR-MS standard data product and a PTR-MS exploratory data product (definition and details are given in chapter 3). The standard data product has been made publicly available as hourly average volume mixing ratios in NILU's EBAS database (<http://ebas.nilu.no>; select "BIRKENES II" and "online_ptr"). Units are given in parts per trillion by volume (pptv, 1 pptv = 10^{-12} v/v).

3 Results

3.1 Full mass spectrum analysis

The automated peak search analysis detected 211 signals in the PTR-ToF-MS raw spectra recorded at Birkenes. 99 signals (listed in Table 1) were statistically significantly enhanced when the instrumental background was subtracted.

Table 1: List of m/z-signals that were statistically significantly enhanced when the instrumental background was subtracted from the PTR-ToF-MS raw spectra recorded at the Birkenes Observatory.

m/z range	Detected signals
30-40	31.017; 33.033
40-50	41.039; 42.035 ; 43.025; 43.055; 44.000; 44.026; 45.032 ; 45.992; 46.029; <i>47.012</i>
50-60	51.042; 52.000; 53.003; 54.034; 57.037; 57.070; 58.031; 58.072; 59.048
60-70	60.044; <i>61.028</i> ; 62.028; 63.028 ; 65.021; 68.996; 69.034; 69.070
70-80	71.049 , 71.085; 72.045; 72.085; 73.028; 73.065 ; 74.024; 74.069; 75.033; 75.044; 79.012; 79.054
80-90	80.990; 81.035; 81.070; 82.945; 83.048; 83.080; 85.030; 85.103; 87.007; 87.044; <i>87.080</i> ; 88.076; <i>89.060</i>
90-100	93.004; 93.069 ; 96.962; 97.037; 97.099; 98.956; 99.008; 99.044; 99.081
100-110	100.040; 100.935; 101.023; 101.061; <i>101.098</i> ; 102.936; 103.073; 107.085
110-120	113.023; 113.060; 115.075; 116.904; 118.902
120-130	120.900; 121.103 ; 123.942; 124.072; 129.071
130-140	130.990; 135.118; 137.133 ; 139.064; 139.111
140-150	143.101; 146.977; 148.974
150-160	<i>151.110</i> ; 157.157
160-170	162.998; 169.120
170-180	173.013
180-190	180.938; 182.935
190-200	196.980
200-210	205.198
210-220	212.994

Amongst the 99 signals of interest, we identified/classified 13 signals (Table 1, in bold) as the PTR-MS standard data product while 6 signals (Table 1, italic) were identified/classified as an exploratory PTR-MS data product. These 19 signals were subjected to further analysis and included in this summary report. An analysis of the remaining signals is beyond the scope of this work and should be included in future studies.

Figure 6 displays the relative abundances of all analyte ions with relative abundance greater than 1 % of the total analyte ion signal (i.e. the sum of all detected organic analyte ion signals). The reader is cautioned that signal count

rates (uncalibrated data) have been used for this analysis. The upper panel shows the results from the summer 2012 campaign, the lower panel shows the data measured in winter 2013.

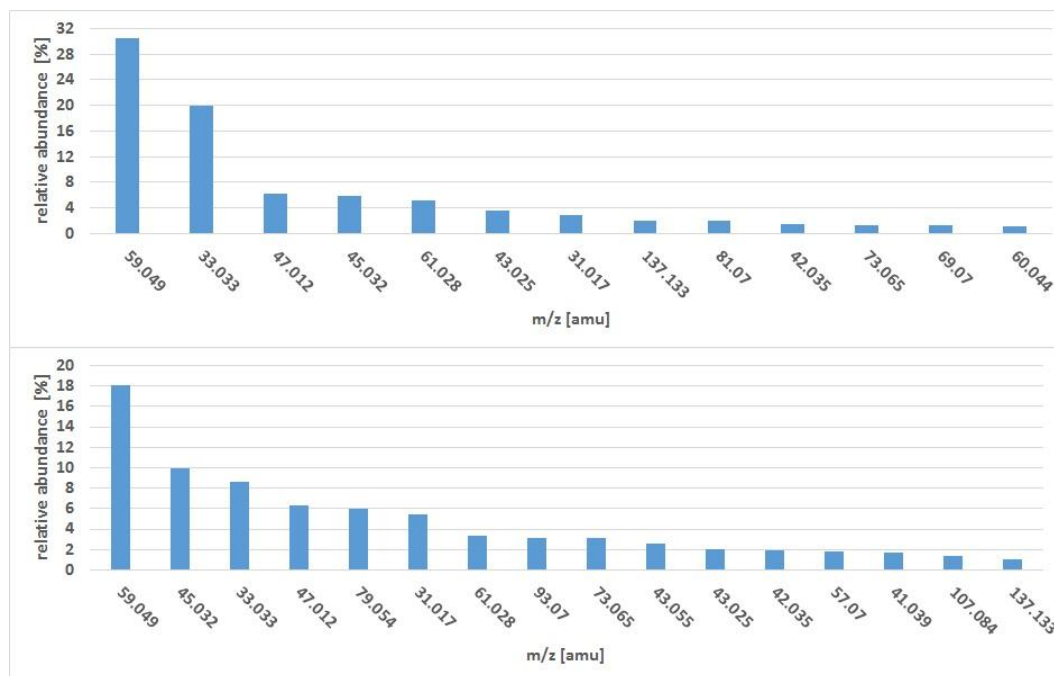


Figure 6: Relative abundances of all analyte ions with relative abundance greater than 1 % of the total analyte ion signal (i.e. the sum of all detected organic analyte ion signals).

The summer spectrum is dominated by oxygenated VOCs (m/z 59.039 and m/z 60.044: acetone; m/z 33.033: methanol; m/z 47.012: formic acid; m/z 45.032: acetaldehyde; m/z 61.028 and m/z 43.025: acetic acid; m/z 31.017: formaldehyde; m/z 73.065: methylethylketone) and biogenic hydrocarbons including monoterpenes (m/z 81.070 and m/z 137.133) and isoprene (m/z 69.070). The m/z 42.035 signal arises from acetonitrile, a long-lived biomass-burning tracer.

The winter spectrum is also dominated by oxygenated VOCs but the contribution from aromatic hydrocarbons (m/z 79.054: benzene; m/z 93.070: toluene; m/z 107.084: C₈-alkylbenzenes) becomes more significant. In addition, we observed a series of unspecific ion fragments (m/z 43.055: C₃H₇⁺; m/z 57.070: C₄H₉⁺; m/z 41.039: C₃H₅⁺).

3.2 PTR-MS standard data product

The PTR-MS technique has been extensively validated for atmospheric VOC measurements (e.g. deGouw and Warneke, 2007). These validation exercises have resulted in a set of m/z -signals that can be specifically assigned to organic trace gases in the troposphere. We herein refer to this set of signals as the PTR-MS standard data product. Highly mass-resolved measurements by PTR-ToF-MS have narrowed down the list of known interferants in the standard data product specified in Table 2. As mentioned above, the PTR-MS standard data product has

been made available as hourly average volume mixing ratios in NILU's EBAS database. The m/z 63.028 (DMS) and m/z 73.065 (MEK) signals have not yet been included in the database as they warrant further validation.

Table 2: List of m/z -signals that can be specifically assigned to organic trace gases in the remote troposphere (PTR-MS standard data product).

m/z	Ion sum formula	Neutral precursor	Calibration	known interferants^a
33.033	CH ₅ O ⁺	methanol	certified standard	--
42.035	C ₂ H ₄ N ⁺	acetonitrile	certified standard	--
45.032	C ₂ H ₅ O ⁺	acetaldehyde	certified standard	--
59.048	C ₃ H ₇ O ⁺	acetone	certified standard	propanal
63.028	C ₂ H ₇ S ⁺	dimethyl sulphide (DMS)	data from previous campaign	--
69.070	C ₅ H ₉ ⁺	isoprene	certified standard	2-methyl-3-buten-2-ol (MBO)
71.049	C ₄ H ₇ O ⁺	methylvinylketone (MVK) methacrolein (MACR)	acetone sensitivity used as proxy	other low-NO _x isoprene oxidation products
73.065	C ₄ H ₇ O ⁺	methylethylketone (MEK)	certified standard	butanal
79.054	C ₆ H ₇ ⁺	benzene	certified standard	
93.069	C ₇ H ₉ ⁺	toluene	certified standard	cymene
107.085	C ₈ H ₁₁ ⁺	C ₈ -alkylbenzenes (sum of isomers)	certified standard of p-xylene	
121.103	C ₉ H ₁₃ ⁺	C ₉ -alkylbenzenes (sum of isomers)	certified standard of 1,3,5-TMB	
137.133	C ₁₀ H ₁₇ ⁺	monoterpenes (sum of isomers)	certified standard of α -pinene	linalool sesquiterpenes

^a includes only compounds potentially present at remote forested sites

At this stage of the analysis, we will only present the data and provide a basic statistical description. For each m/z -signal we will, in the following, report¹

- i) the time series as measured during the summer 2012 and the winter 2013 campaign, respectively
- ii) the monthly averaged diurnal cycle as measured during the months of May, June, July and August in 2012 and the months of January and February in 2013 (8 days only in February)

¹ The reader is cautioned that the acetone, isoprene, MVK+MACR, MEK, toluene and monoterpene data may be positively biased due to potential interferences (Table 2). Any conclusions drawn from these data must consider a potential bias from interferant species.

- iii) a box-and-whisker plot statistical analysis performed on hourly mean values for each month, the median being shown as the black band within the gray first and third quartiles and the ends of the whiskers representing mild outliers up to a maximum of 3*IQR (interquartile range).

When viewing the summer time plot, the reader is pointed to an episode of interest in late May 2012 when sustained air temperatures over 20 °C were reached during the vegetation growing season. All oxygenated VOCs peaked during this period, either due to strong direct biogenic emissions and/or due to increased secondary photochemical formation in the atmosphere. This was also the period when the highest ozone levels ($\sim 130 \mu\text{g}/\text{m}^3$) of the entire year 2012 were recorded at Birkenes. We identify this episode as of particular interest for future analyses.

3.2.1 m/z 33.033 (methanol)

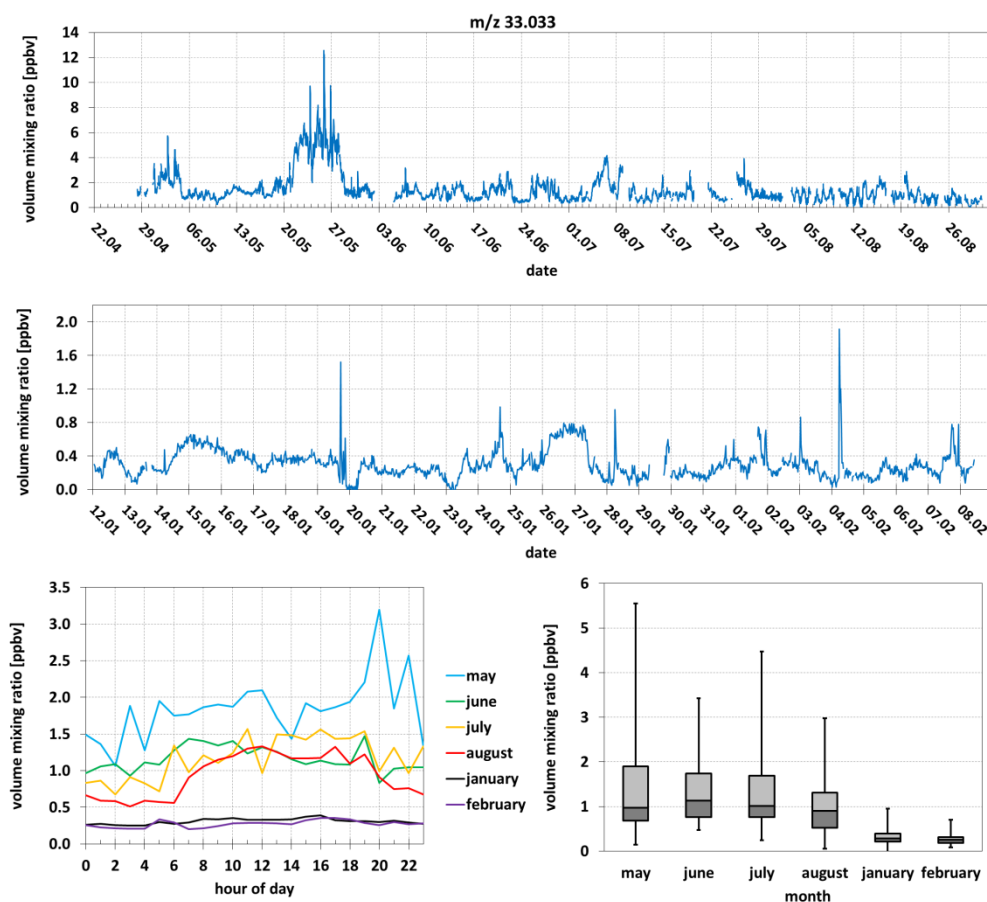


Figure 7: Time series of the m/z 33.003 signal (methanol) as observed during the summer 2012 (upper panel) and winter 2013 (central panel); monthly averaged diurnal cycle as measured during May 2012, June 2012, July 2012, August 2012, January 2013 and February 2013 (lower left panel); box-and-whisker plot of a monthly statistical analysis on hourly mean values (lower right panel).

3.2.2 m/z 42.035 (acetonitrile)

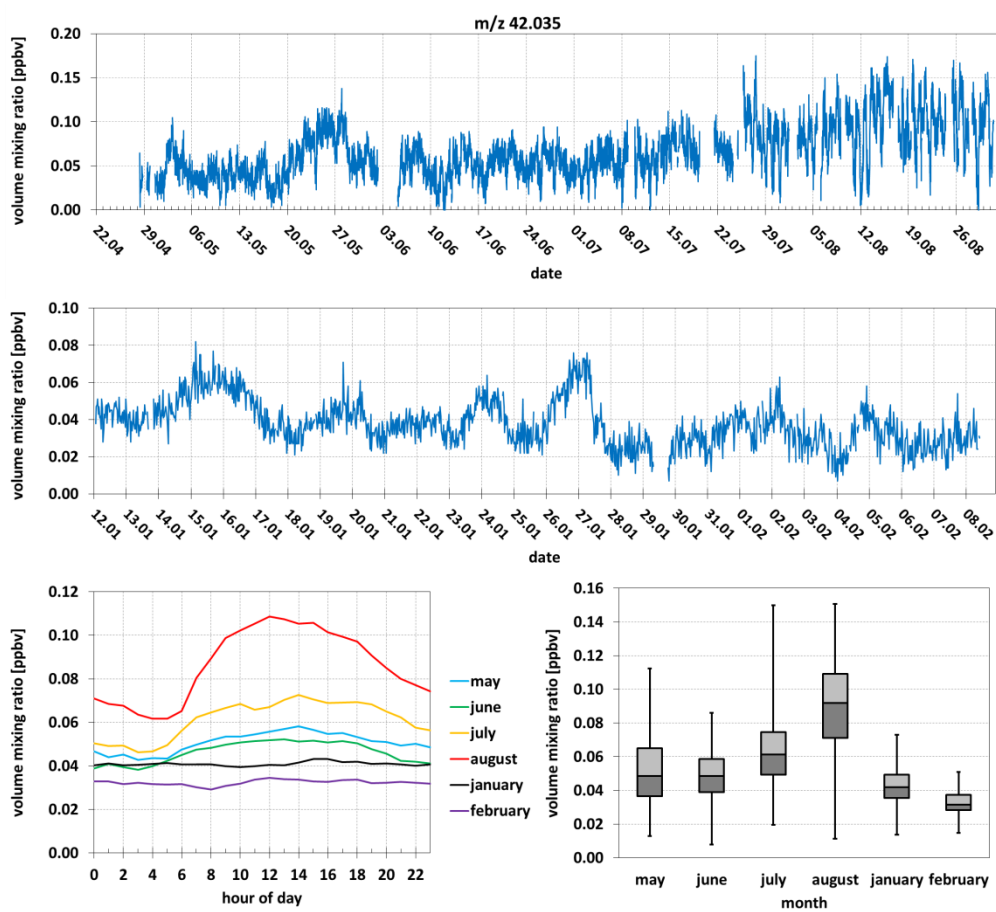


Figure 8: Time series of the m/z 42.035 signal (acetonitrile) as observed during the summer 2012 (upper panel) and winter 2013 (central panel); monthly averaged diurnal cycle as measured during May 2012, June 2012, July 2012, August 2012, January 2013 and February 2013 (lower left panel); box-and-whisker plot of a monthly statistical analysis on hourly mean values (lower right panel).

3.2.3 m/z 45.032 (acetaldehyde)

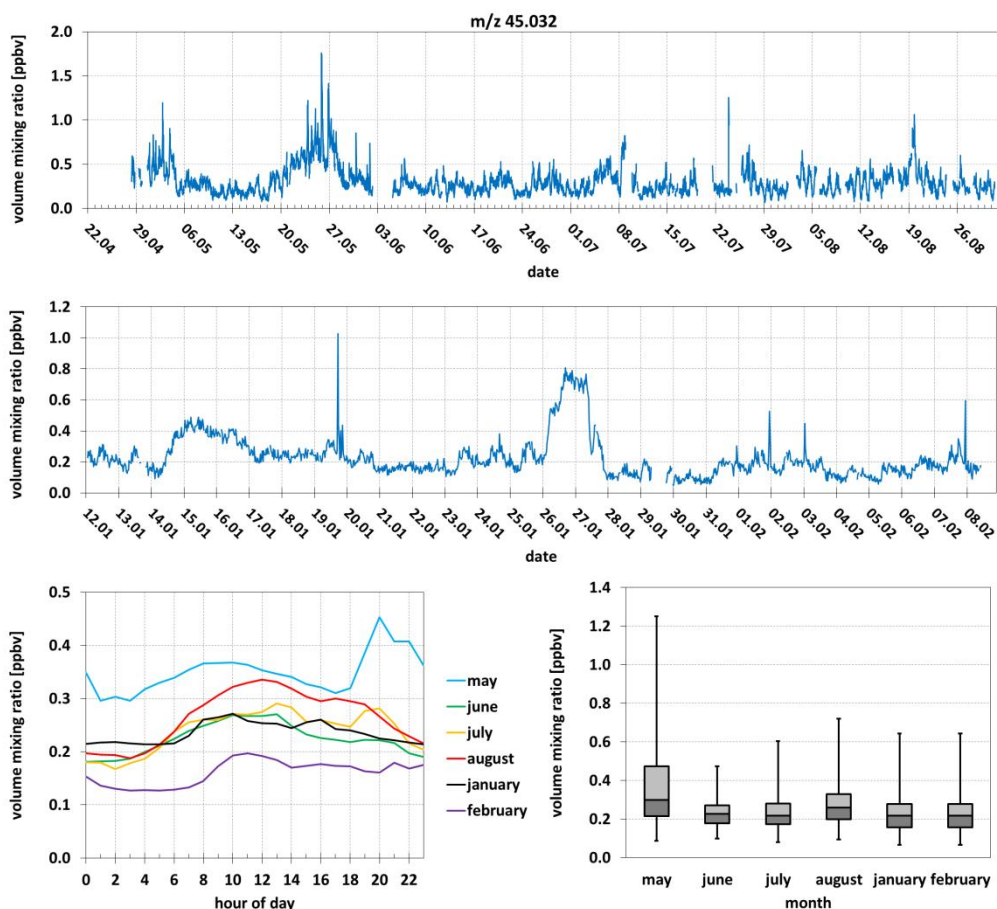


Figure 9: Time series of the m/z 45.032 signal (acetaldehyde) as observed during the summer 2012 (upper panel) and winter 2013 (central panel); monthly averaged diurnal cycle as measured during May 2012, June 2012, July 2012, August 2012, January 2013 and February 2013 (lower left panel); box-and-whisker plot of a monthly statistical analysis on hourly mean values (lower right panel).

3.2.4 m/z 59.048 (acetone)

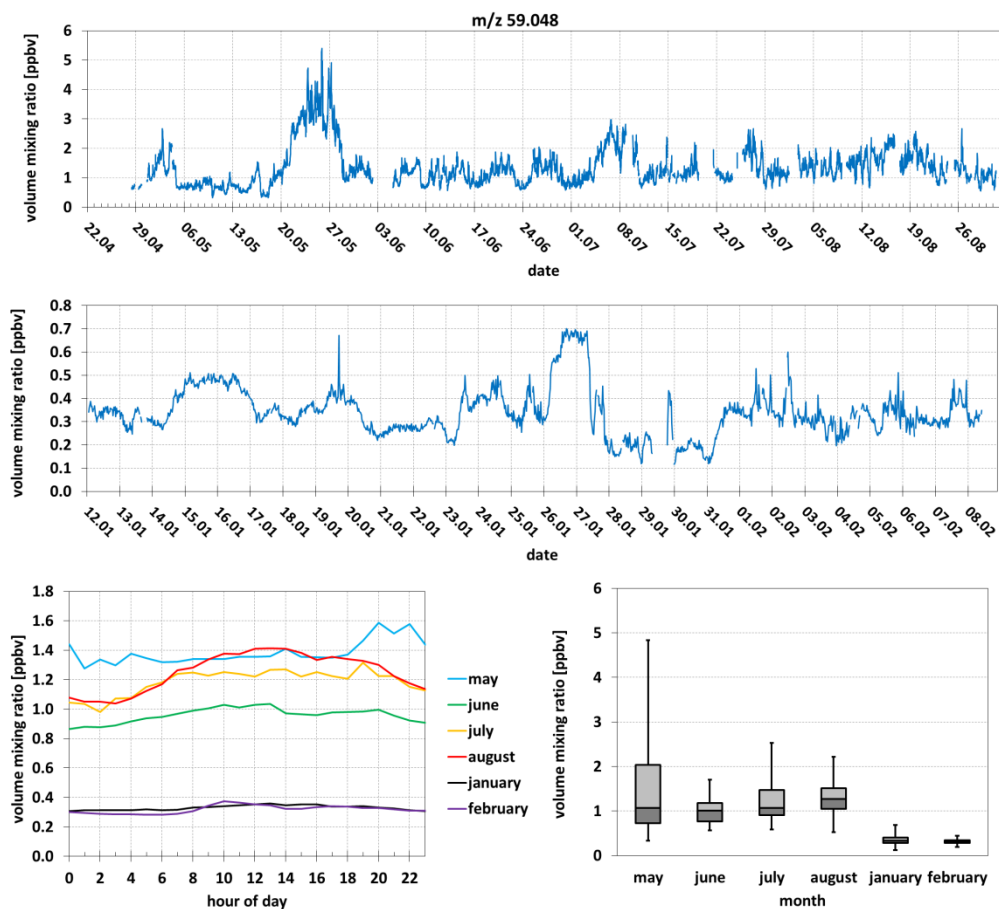


Figure 10: Time series of the m/z 59.048 signal (acetone) as observed during the summer 2012 (upper panel) and winter 2013 (central panel); monthly averaged diurnal cycle as measured during May 2012, June 2012, July 2012, August 2012, January 2013 and February 2013 (lower left panel); box-and-whisker plot of a monthly statistical analysis on hourly mean values (lower right panel).

3.2.5 m/z 63.028 (dimethyl sulphide)

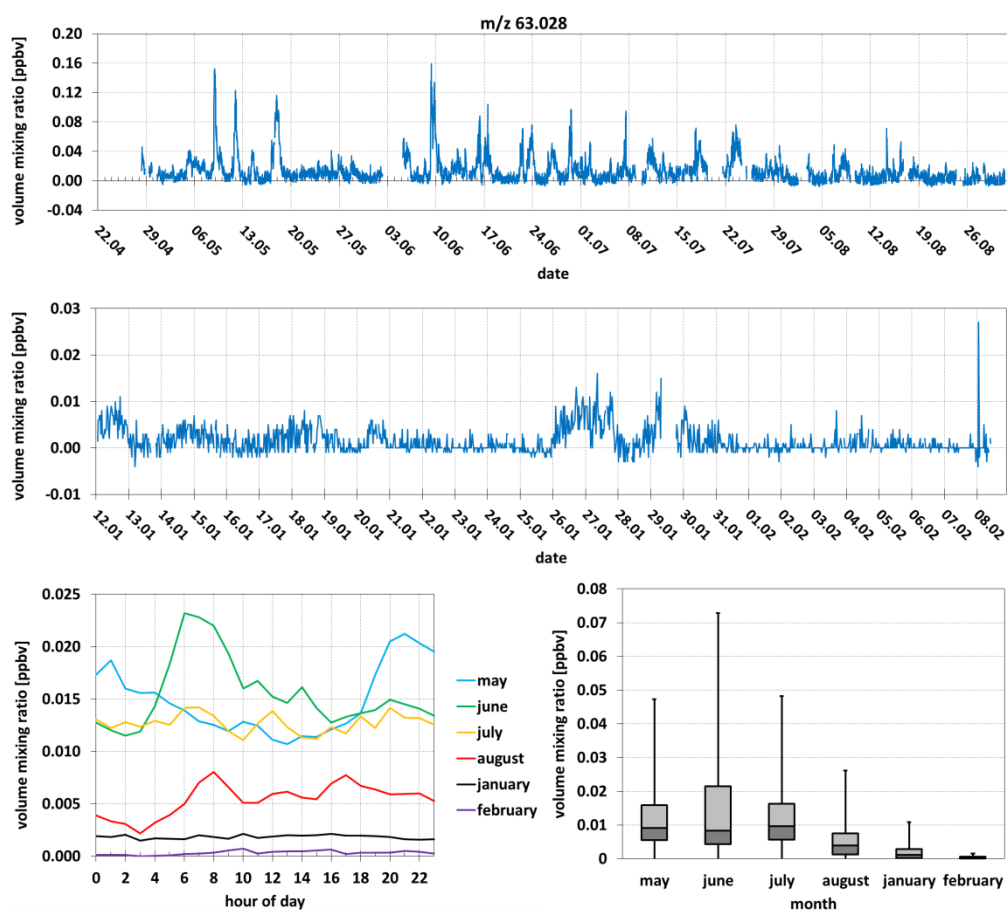


Figure 11: Time series of the m/z 63.028 signal (dimethyl sulphide) as observed during the summer 2012 (upper panel) and winter 2013 (central panel); monthly averaged diurnal cycle as measured during May 2012, June 2012, July 2012, August 2012, January 2013 and February 2013 (lower left panel); box-and-whisker plot of a monthly statistical analysis on hourly mean values (lower right panel).

3.2.6 m/z 69.070 (isoprene)

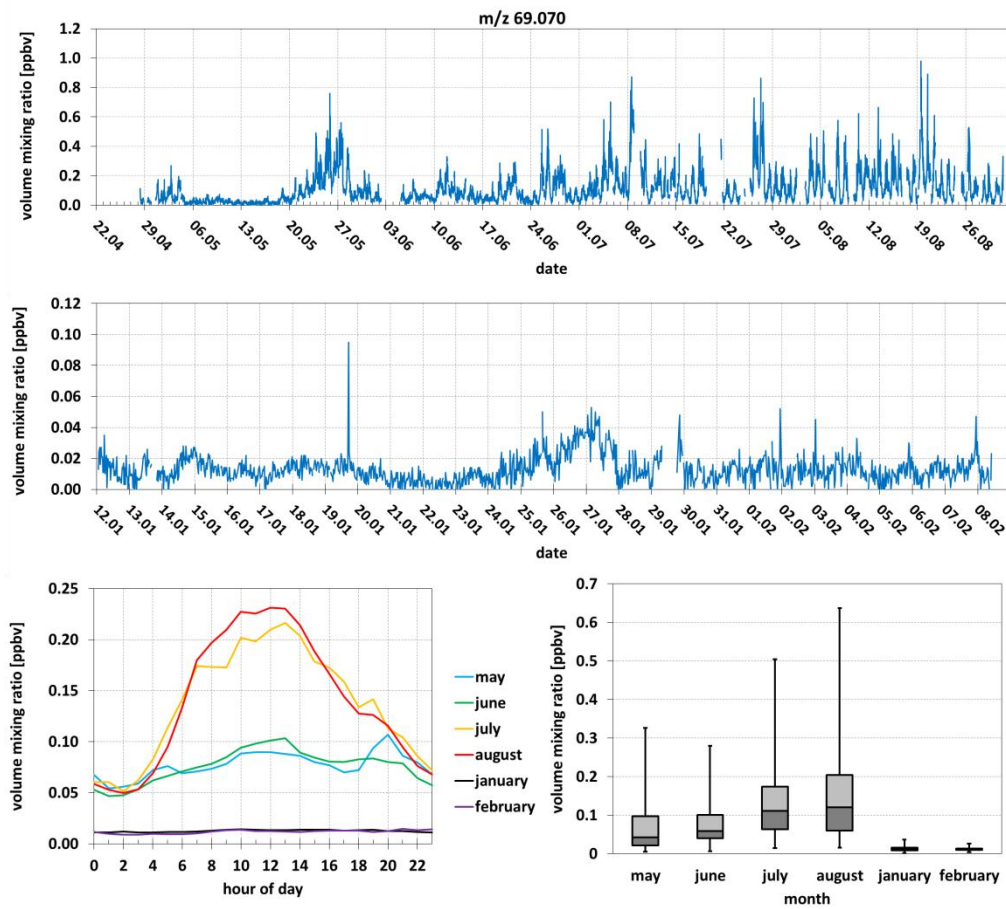


Figure 12: Time series of the m/z 69.070 signal (isoprene) as observed during the summer 2012 (upper panel) and winter 2013 (central panel); monthly averaged diurnal cycle as measured during May 2012, June 2012, July 2012, August 2012, January 2013 and February 2013 (lower left panel); box-and-whisker plot of a monthly statistical analysis on hourly mean values (lower right panel).

3.2.7 m/z 71.049 (sum of methylvinylketone and methacrolein)

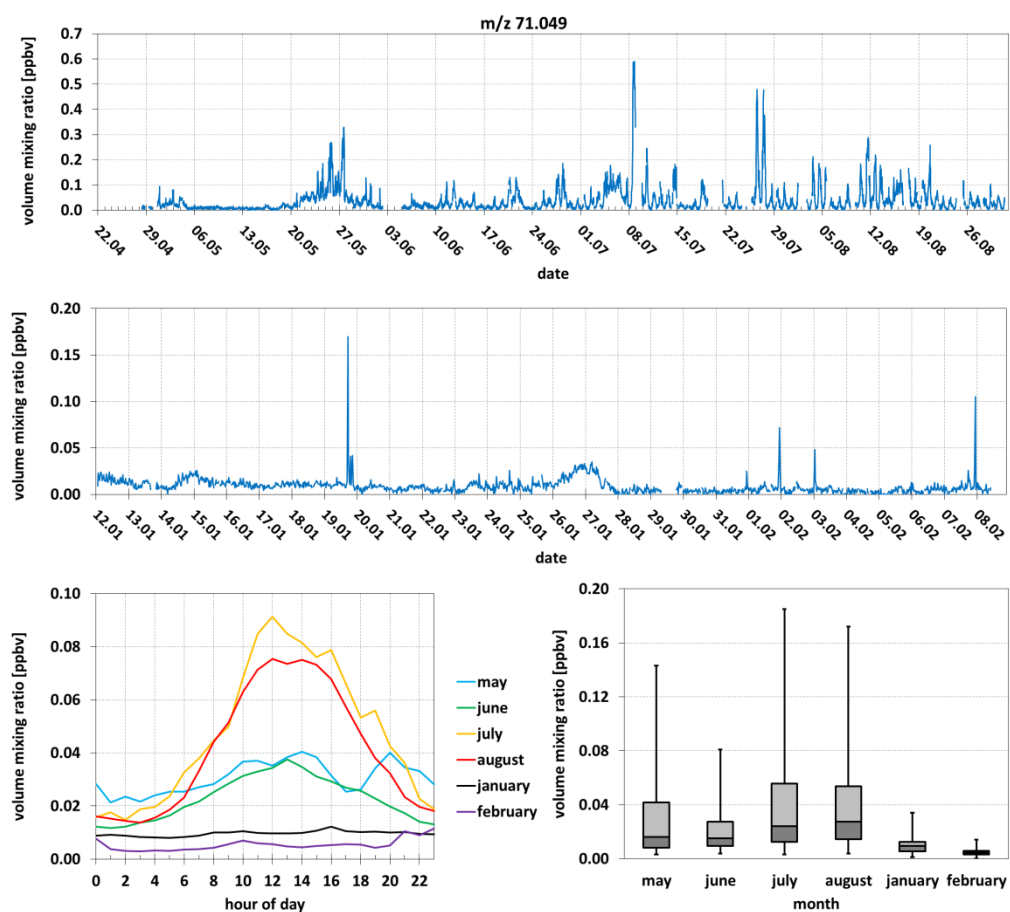


Figure 13: Time series of the m/z 71.049 (sum of methylvinylketone and methacrolein) signal as observed during the summer 2012 (upper panel) and winter 2013 (central panel); monthly averaged diurnal cycle as measured during May 2012, June 2012, July 2012, August 2012, January 2013 and February 2013 (lower left panel); box-and-whisker plot of a monthly statistical analysis on hourly mean values (lower right panel).

3.2.8 m/z 73.065 (methylethylketone)

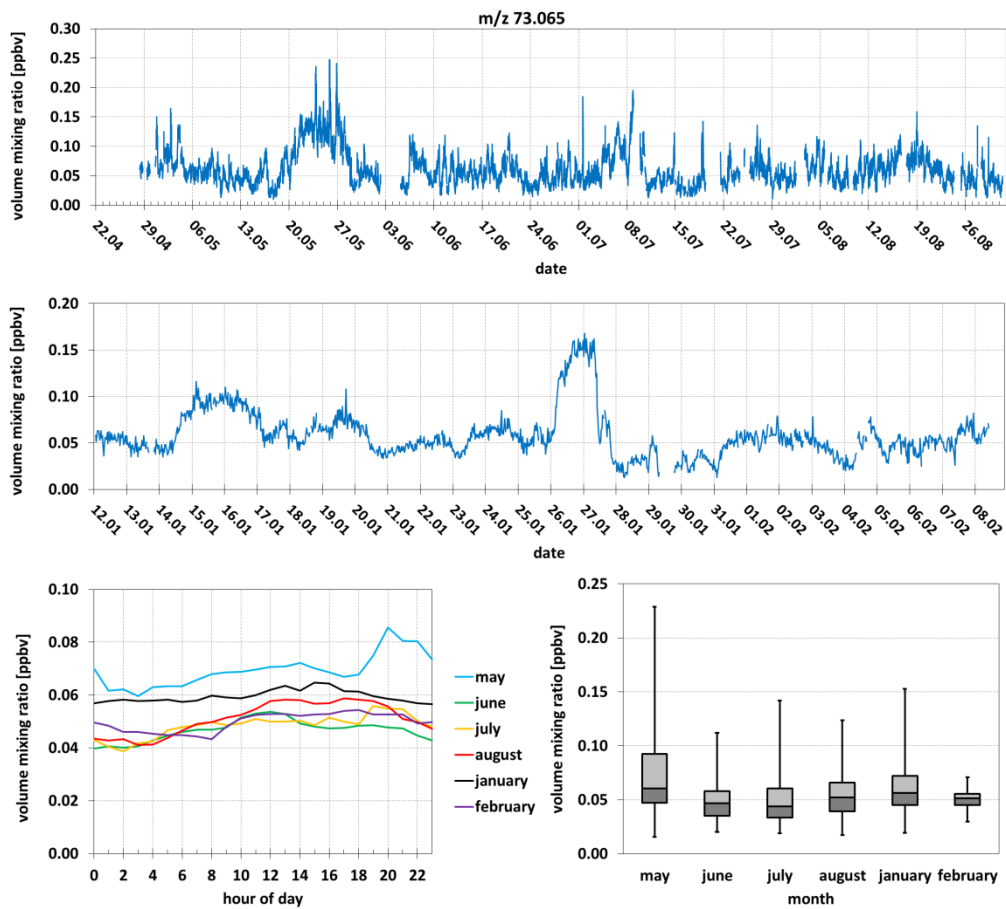


Figure 14: Time series of the m/z 73.065 (methylethylketone) signal as observed during the summer 2012 (upper panel) and winter 2013 (central panel); monthly averaged diurnal cycle as measured during May 2012, June 2012, July 2012, August 2012, January 2013 and February 2013 (lower left panel); box-and-whisker plot of a monthly statistical analysis on hourly mean values (lower right panel).

3.2.9 m/z 79.054 (benzene)

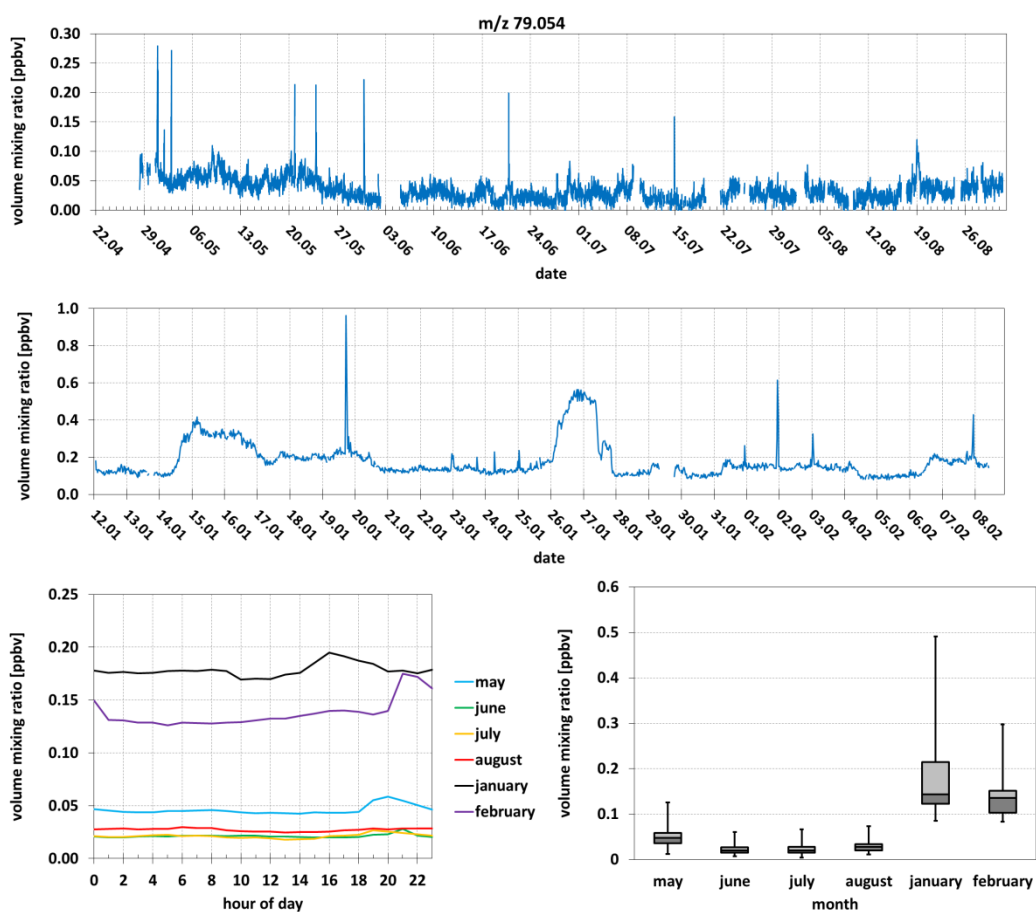


Figure 15: Time series of the m/z 79.054 signal (benzene) as observed during the summer 2012 (upper panel) and winter 2013 (central panel); monthly averaged diurnal cycle as measured during May 2012, June 2012, July 2012, August 2012, January 2013 and February 2013 (lower left panel); box-and-whisker plot of a monthly statistical analysis on hourly mean values (lower right panel).

3.2.10 m/z 93.069 (toluene)

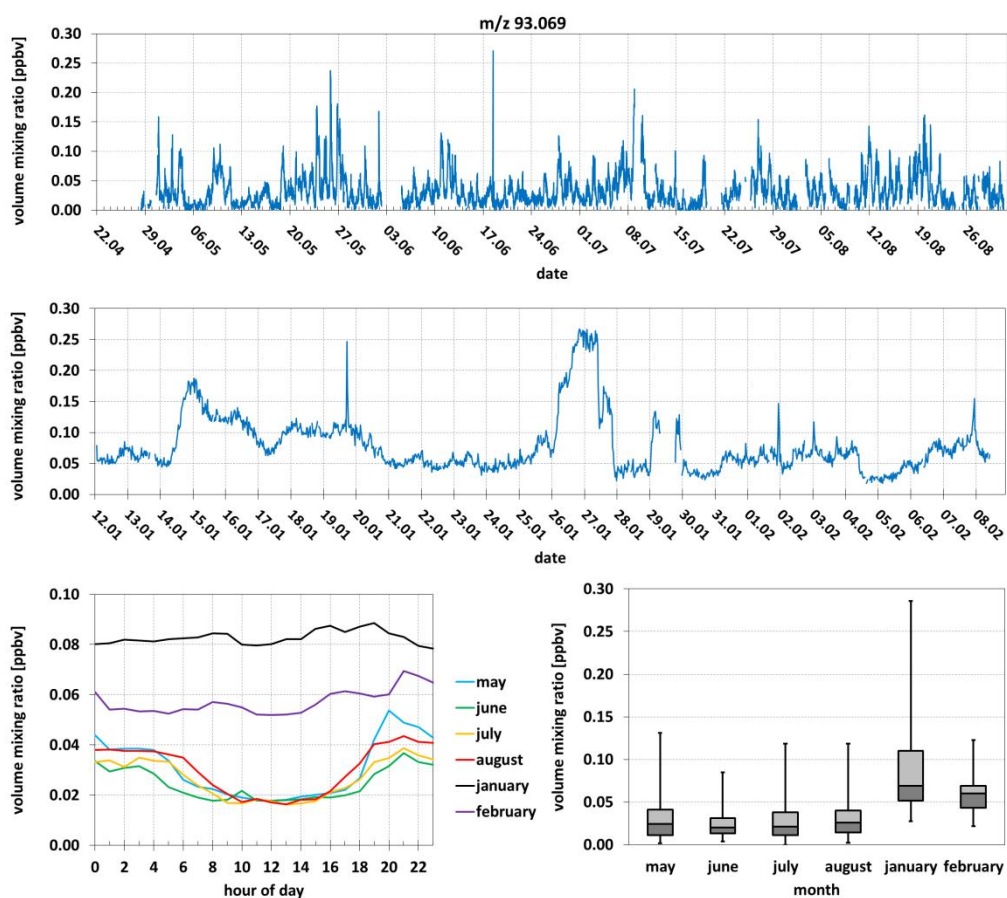


Figure 16: Time series of the m/z 93.069 signal (toluene) as observed during the summer 2012 (upper panel) and winter 2013 (central panel); monthly averaged diurnal cycle as measured during May 2012, June 2012, July 2012, August 2012, January 2013 and February 2013 (lower left panel); box-and-whisker plot of a monthly statistical analysis on hourly mean values (lower right panel).

3.2.11 m/z 107.085 (sum of C_8 -alkylbenzene isomers)

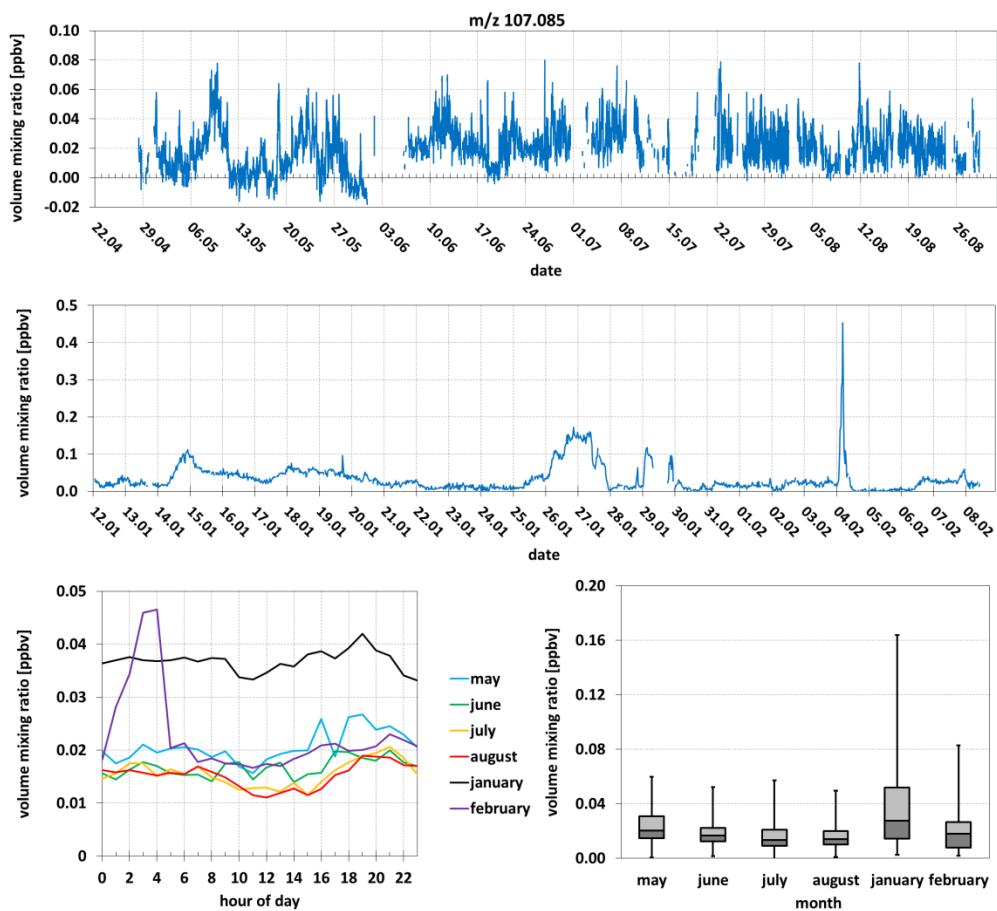


Figure 17: Time series of the m/z 107.085 signal (C_8 -alkylbenzenes) as observed during the summer 2012 (upper panel) and winter 2013 (central panel); monthly averaged diurnal cycle as measured during May 2012, June 2012, July 2012, August 2012, January 2013 and February 2013 (lower left panel); box-and-whisker plot of a monthly statistical analysis on hourly mean values (lower right panel).

3.2.12 m/z 121.103 (sum of C_9 -alkylbenzene isomers)

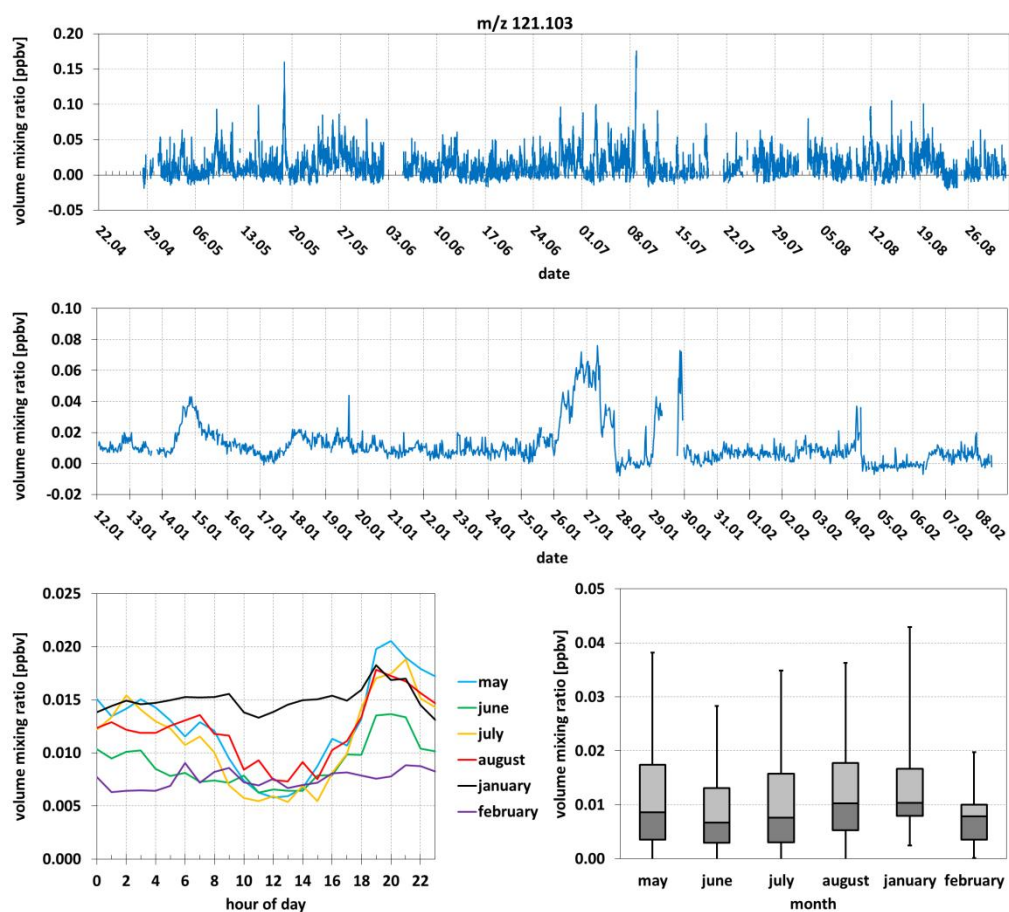


Figure 18: Time series of the m/z 121.103 signal (C_9 -alkylbenzenes) as observed during the summer 2012 (upper panel) and winter 2013 (central panel); monthly averaged diurnal cycle as measured during May 2012, June 2012, July 2012, August 2012, January 2013 and February 2013 (lower left panel); box-and-whisker plot of a monthly statistical analysis on hourly mean values (lower right panel).

3.2.13 m/z 137.133 (sum of monoterpene isomers)

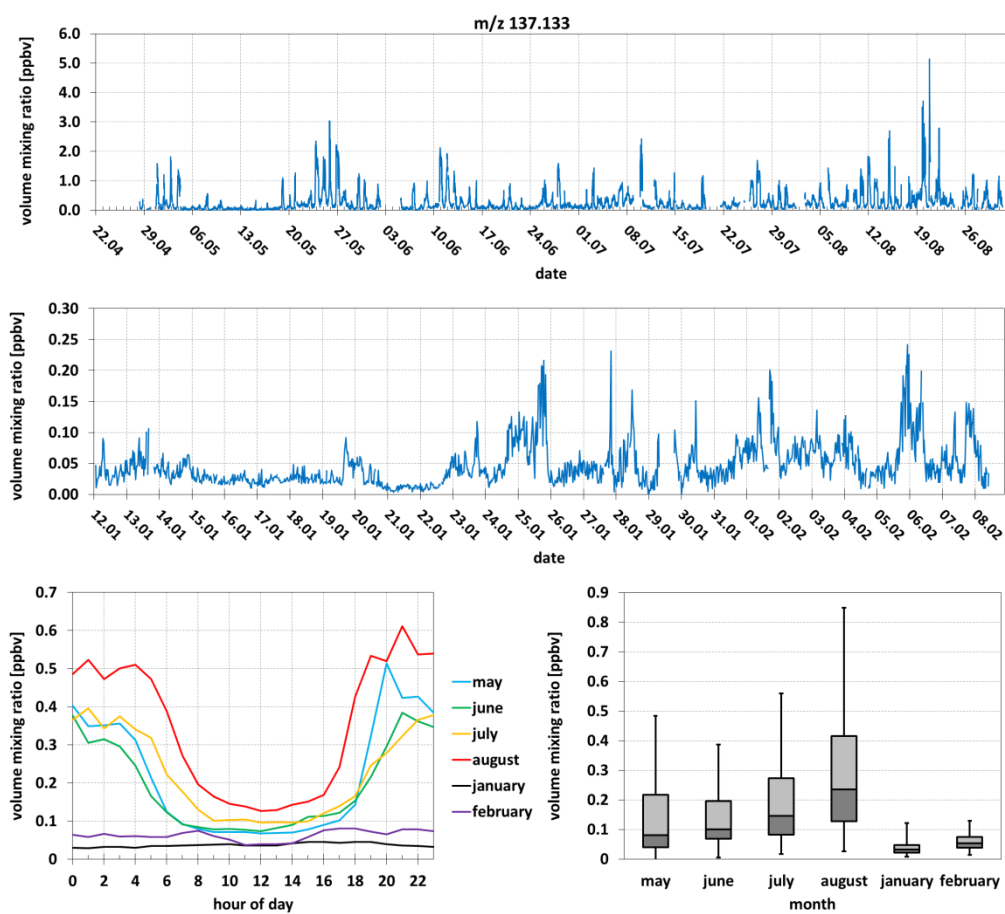


Figure 19: Time series of the m/z 137.133 signal (sum of monoterpene isomers) as observed during the summer 2012 (upper panel) and winter 2013 (central panel); monthly averaged diurnal cycle as measured during May 2012, June 2012, July 2012, August 2012, January 2013 and February 2013 (lower left panel); box-and-whisker plot of a monthly statistical analysis on hourly mean values (lower right panel).

3.3 PTR-MS exploratory data product

A series of recent studies suggest that formic acid and acetic acid can be quantitatively detected by PTR-MS / PTR-ToF-MS at m/z 47.012 and m/z 61.028. However, zeroing and calibration is problematic for both compounds, and in the case of acetic acid, it is not clear to what extent the isomeric species glycolaldehyde and methyl formate act as interferants in the remote troposphere.

Previous work also indicates that pinonaldehyde, the major atmospheric oxidation product of α -pinene, is detected at m/z 151.110. An accurate quantification is, however, only possible if a pure authentic sample is available.

Finally, the ion signals at m/z 87.080, m/z 89.060 and m/z 101.098 or their nominal m/z equivalents are commonly present in PTR-ToF-MS and PTR-MS mass spectra recorded in biogenically impacted air. To date it is not clear what the neutral precursors of these signals are.

Herein we report these 6 signals as PTR-MS exploratory product (Table 3). The term exploratory means that the identification and/or quantification of these signals are tentative at the current state of knowledge.

Table 3: List of m/z -signals that have been tentatively identified and quantified.

m/z	Ion sum formula	Neutral precursor	Calibration	Known interferants
47.012	CH ₃ O ₂ ⁺	formic acid	ion-molecule reaction kinetics	--
61.028	C ₂ H ₅ O ₂ ⁺	acetic acid	ion-molecule reaction kinetics	glycolaldehyde methyl formate
87.080	C ₅ H ₁₁ O ⁺	unidentified	acetone sensitivity used as proxy (purely indicative quantification)	
89.060	C ₄ H ₉ O ₂ ⁺	unidentified	acetone sensitivity used as proxy (purely indicative quantification)	
101.098	C ₆ H ₁₃ O ⁺	unidentified (hexanal)	acetone sensitivity used as proxy (purely indicative quantification)	
151.110	C ₁₀ H ₁₅ O ⁺	pinonaldehyde	acetone sensitivity used as proxy (purely indicative quantification)	

3.3.1 m/z 47.012 (formic acid)

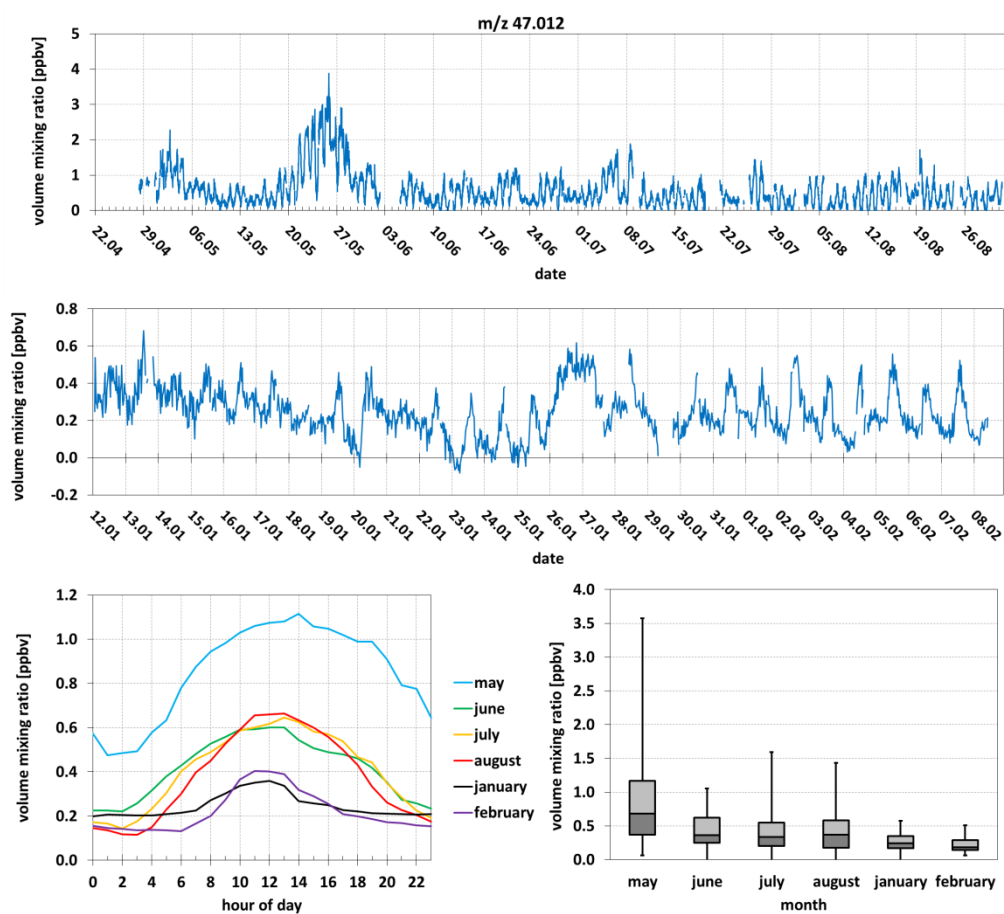


Figure 20: Time series of the m/z 47.012 signal (formic acid) as observed during the summer 2012 (upper panel) and winter 2013 (central panel); monthly averaged diurnal cycle as measured during May 2012, June 2012, July 2012, August 2012, January 2013 and February 2013 (lower left panel); box-and-whisker plot of a monthly statistical analysis on hourly mean values (lower right panel).

3.3.2 m/z 61.028 (acetic acid)

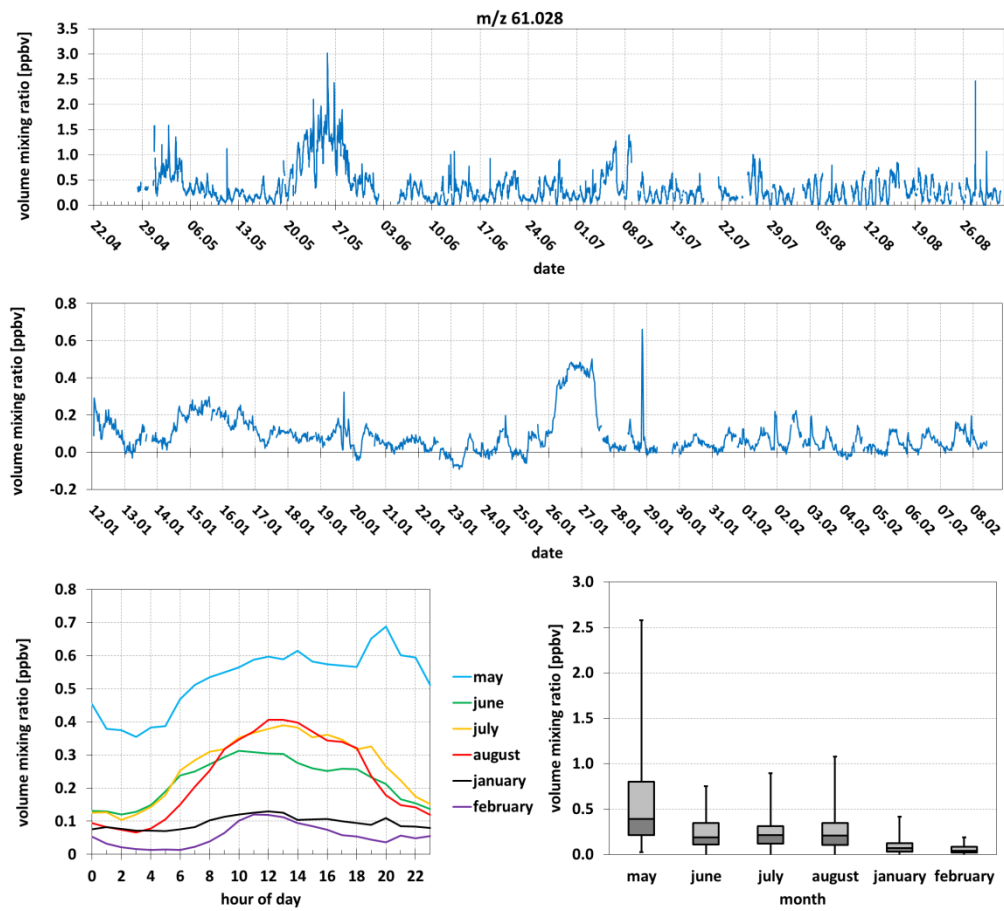


Figure 21: Time series of the m/z 61.028 signal (acetic acid) as observed during the summer 2012 (upper panel) and winter 2013 (central panel); monthly averaged diurnal cycle as measured during May 2012, June 2012, July 2012, August 2012, January 2013 and February 2013 (lower left panel); box-and-whisker plot of a monthly statistical analysis on hourly mean values (lower right panel).

3.3.3 m/z 87.080 (unidentified)

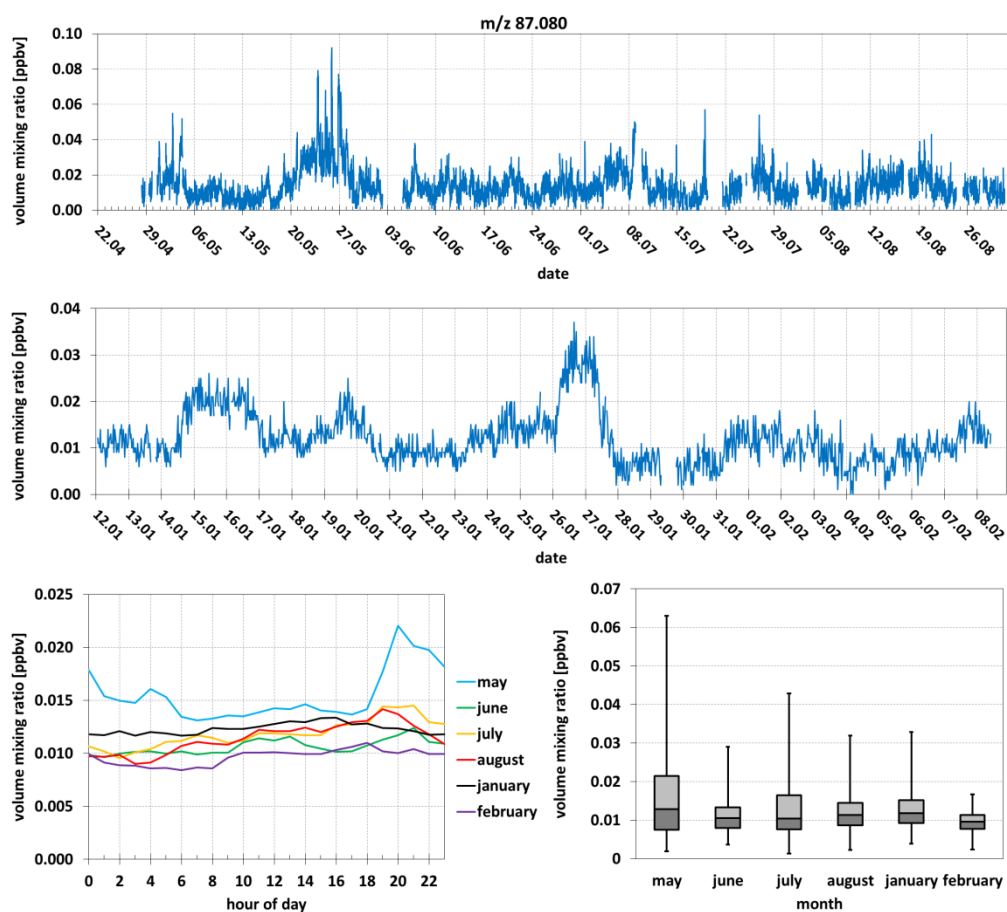


Figure 22: Time series of the m/z 87.080 signal (unidentified) as observed during the summer 2012 (upper panel) and winter 2013 (central panel); monthly averaged diurnal cycle as measured during May 2012, June 2012, July 2012, August 2012, January 2013 and February 2013 (lower left panel); box-and-whisker plot of a monthly statistical analysis on hourly mean values (lower right panel).

3.3.4 m/z 89.060 (unidentified)

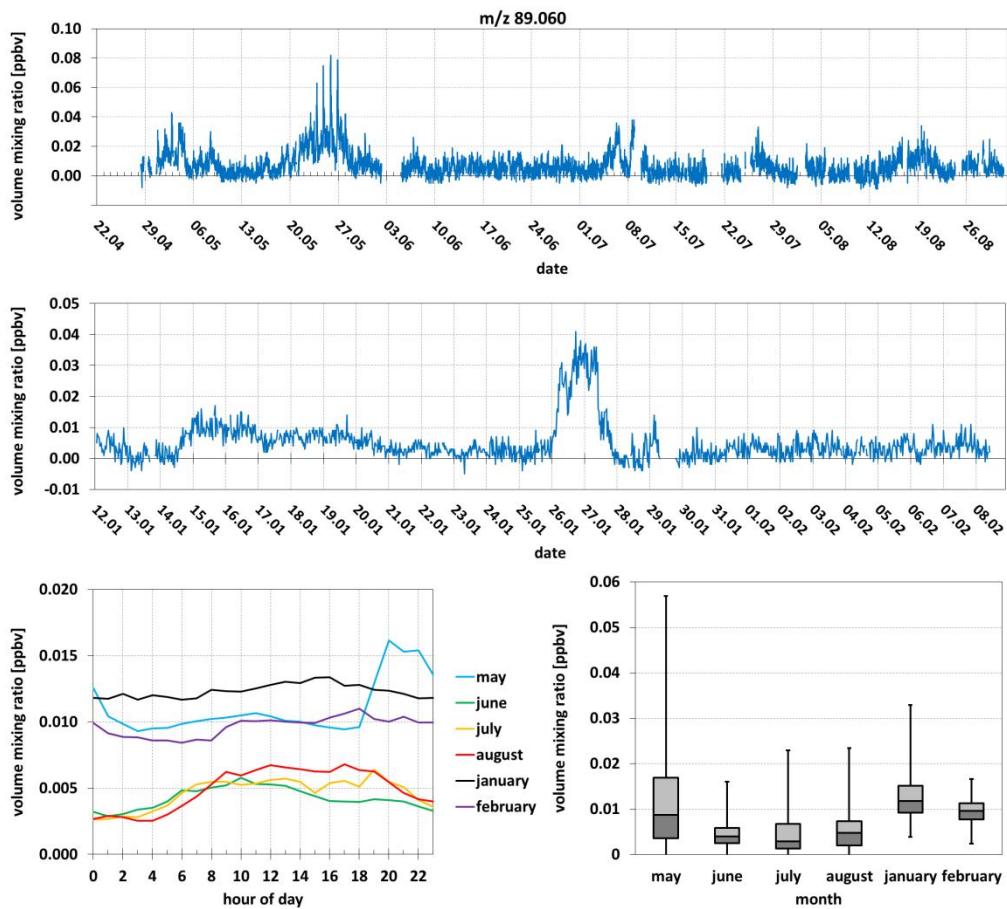


Figure 23: Time series of the m/z 89.060 signal (unidentified) as observed during the summer 2012 (upper panel) and winter 2013 (central panel); monthly averaged diurnal cycle as measured during May 2012, June 2012, July 2012, August 2012, January 2013 and February 2013 (lower left panel); box-and-whisker plot of a monthly statistical analysis on hourly mean values (lower right panel).

3.3.5 m/z 101.098 (unidentified)

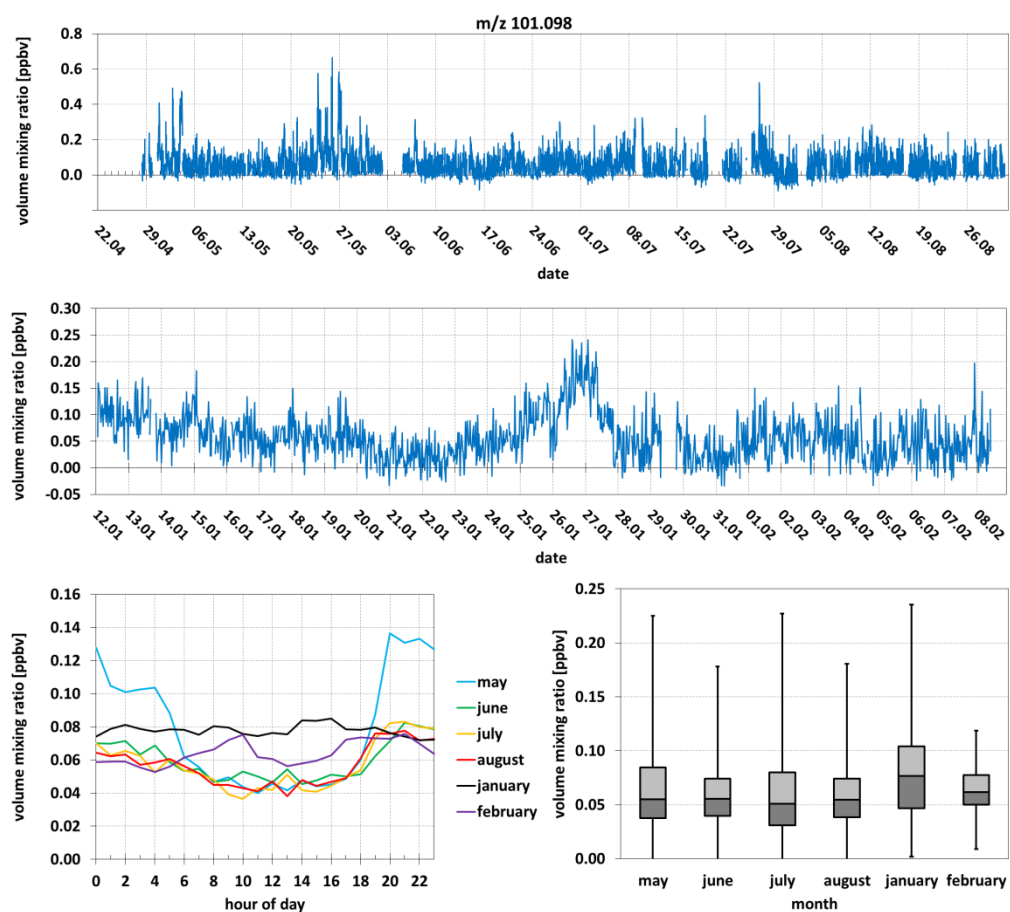


Figure 24: Time series of the m/z 101.098 signal (unidentified) as observed during the summer 2012 (upper panel) and winter 2013 (central panel); monthly averaged diurnal cycle as measured during May 2012, June 2012, July 2012, August 2012, January 2013 and February 2013 (lower left panel); box-and-whisker plot of a monthly statistical analysis on hourly mean values (lower right panel).

3.3.6 m/z 151.110 (pinonaldehyde)

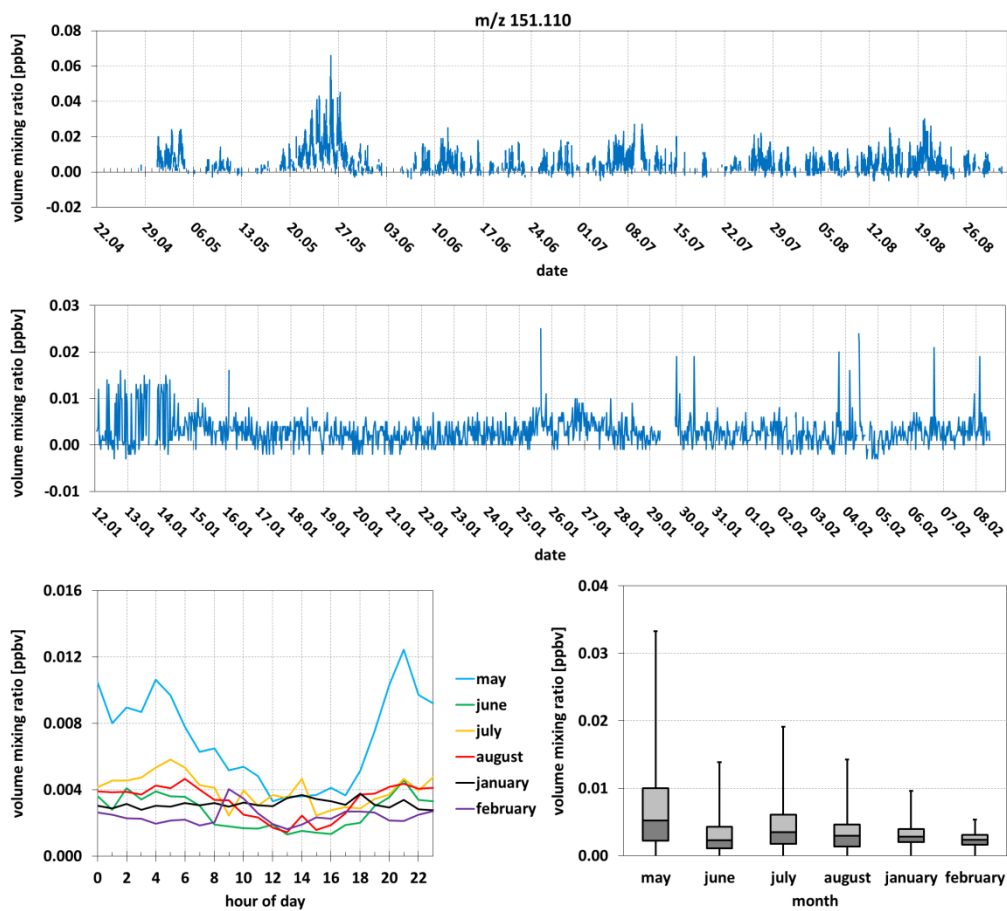


Figure 25: Time series of the m/z 151.110 signal (pinonaldehyde) as observed during the summer 2012 (upper panel) and winter 2013 (central panel); monthly averaged diurnal cycle as measured during May 2012, June 2012, July 2012, August 2012, January 2013 and February 2013 (lower left panel); box-and-whisker plot of a monthly statistical analysis on hourly mean values (lower right panel).

3.4 A preliminary analysis of the monoterpenes and isoprene data

Our initial data analysis and interpretation has focused on the phenomenology of monoterpene and isoprene variations. Figure 26 shows the mean diurnal cycle of monoterpenes (upper panel) and isoprene (lower panel) as observed at the Birkenes Observatory through the months of May, June, July and August 2012 and January and February 2013.

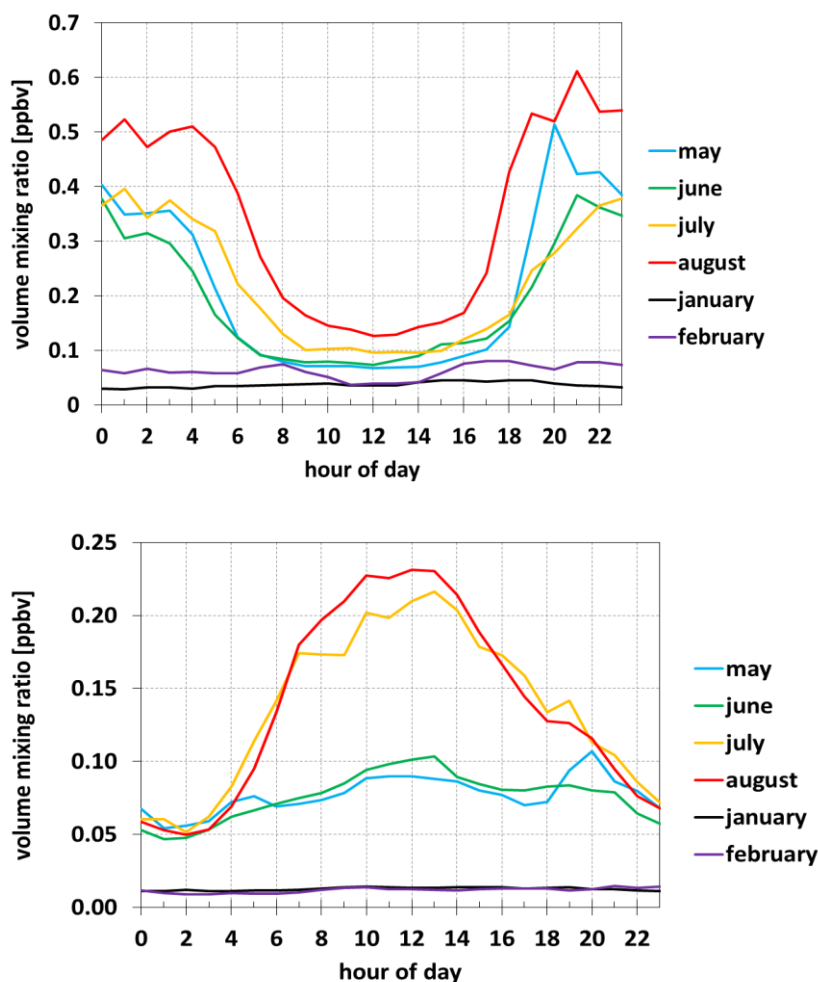


Figure 26: Monthly averaged diurnal cycle of monoterpenes (upper panel) and isoprene (lower panel) as observed at the Birkenes Observatory.

Not unexpectedly, significant levels of monoterpenes and isoprene were only detected during the warm summer months.

Highest mean levels were observed in August when monoterpenes reached nighttime maxima of 0.5 to 0.6 ppbv and isoprene levels peaked during daytime at around 0.22 ppbv. It is pointed out that these values refer to monthly mean averages. Hourly mean maxima of monoterpenes and isoprene reached levels up to 3 ppbv and 0.9 ppbv, respectively.

For comparison, we show the diurnal cycles of monoterpenes and isoprene as observed in Hyytiälä in Southern Finland (Ruuskanen et al., 2009) (Figure 27). Winter data include observations from December to February, spring data include observations from March to May and summer data cover the period from June to August. Monoterpene observations in Birkenes closely resemble monoterpene observations in Hyytiälä, both in terms of absolute concentrations and in the observed diurnal variation. The diurnal cycle of isoprene is, however, remarkably different between the two sites. The strong noontime maximum in July and August in Birkenes may be explained by localized light-driven emissions in the vicinity of the site. Rinne et al. (2005) explained the evening maximum in isoprene at Hyytiälä by the different light environment in summertime at northern latitudes and/or the absence of strong isoprene emitters in the vicinity of the measurement site.

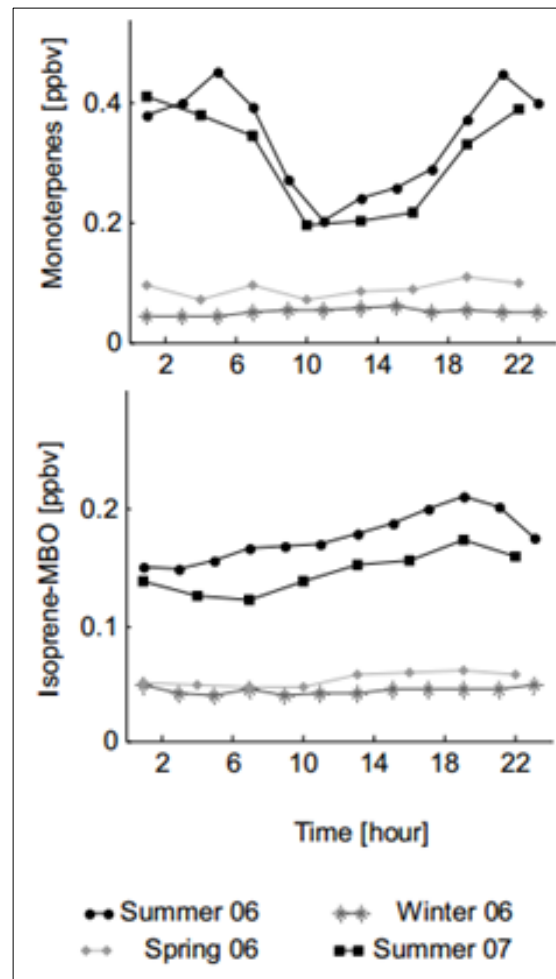


Figure 27: Seasonally averaged diurnal cycle of monoterpenes (upper panel) and isoprene (lower panel) as observed in Hyytiälä, Southern Finland (adapted from Ruuskanen et al., 2009).

Another interesting feature is the anticorrelation in the diurnal cycles of monoterpenes and isoprene in the Birkenes data.

Biogenic emissions of isoprene are strongly light-dependent. The emission results from *de novo* synthesis of isoprene, i.e. there are no storage pools in the plant. Isoprene emissions go to zero at night. This explains the daytime maximum in concentrations and the nighttime minimum.

Monoterpene emissions are temperature-driven and they persist overnight due to release from storage structures. Photo-oxidative losses of monoterpenes are suppressed during nighttime hours.

Figure 28 (left panel) shows the mean diurnal variation in air temperature as recorded at the Birkenes II station in summer 2012 (no May data available). Temperatures typically peaked around 14.00h UTC (local noon).

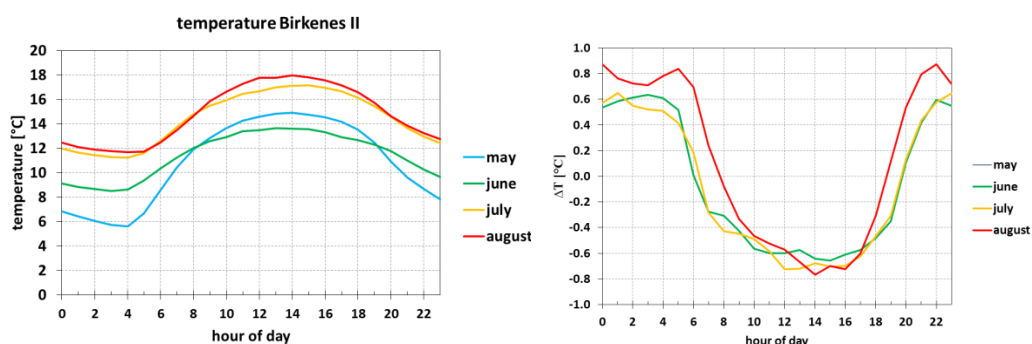


Figure 28: Mean diurnal cycle in air temperature as measured at the Birkenes II station (left panel) and difference between air temperatures measured at the Birkenes II station (219 m asl) and at the Birkenes I station (190 m asl) (right panel).

The right panel of Figure 28 shows the difference between air temperatures measured at the Birkenes II station (219 m asl) and at the Birkenes I station (190 m asl). At local noon, the average air temperature was ~ 0.6 to 0.8 °C higher at the lower Birkenes I station indicating a negative temperature gradient with altitude and well-mixed atmospheric conditions. During nighttime, air temperatures were higher at the more elevated Birkenes II station indicating the formation of a nighttime temperature inversion and suppressed surface layer mixing.

The monoterpene diurnal cycle (which is typical for coniferous forest sites) shows a nighttime maximum due to nighttime emissions from storage pools and weak surface layer mixing.

Future work is warranted to analyze and interpret the collected data on monoterpenes, isoprene, their atmospheric oxidation products and other BVOCs. The data summary provided here confirms that the Birkenes Observatory is an interesting site in the boreo-nemoral vegetation zone where it is possible to

observe both monoterpene and isoprene emissions and photo-chemical processing in the atmosphere. This confirms earlier findings by Yttri et al. (2011) who found both α -pinene and isoprene tracers in SOA collected at Birkenes. Combined chemical measurements of gas phase and particulate phase organics should be carried out in the future.

4 References

- Amundsen, C. E., Hanssen, J. E., Semb, A., Steinnes, E. (1992) Long-range atmospheric transport of trace elements to southern Norway. *Atmos. Environ.*, 26A, 1309–1324.
- De Gouw, J., Warneke, C. (2007) Measurements of volatile organic compounds in the earth's atmosphere using proton-transfer-reaction mass spectrometry. *Mass. Spectrom. Rev.*, 26, 223–257.
- Eckhardt, S., Breivik, K., Li, Y. F., Manø, S., and Stohl, A. (2009) Source regions of some persistent organic pollutants measured in the atmosphere at Birkenes, Norway. *Atmos. Chem. Phys.*, 9, 6597-6610.
- Jordan, A., Haidacher, S., Hanel, G., Hartungen, E., Mark, L., Seehauser, H., Schotchkowsky, R., Sulzer, P., and Mark, T. D.: A high resolution and high sensitivity proton-transfer-reaction time-of-flight mass spectrometer (PTR-TOF-MS). *Int. J. Mass Spectrom.*, 286, 122–128.
- Müller, M., Mikoviny, T., Jud, W., D'Anna, B. and Wisthaler, A. (2013) A new software tool for the analysis of high resolution PTR-TOF mass spectra. *Chemom. Intell. Lab. Syst.*, 127, 158-165.
- Rinne, J., Ruuskanen, T. M., Reissell, A., Taipale, R., Hakola, H., and Kulmala, M. (2005) On-line PTR-MS measurements of atmospheric concentrations of volatile organic compounds in a European boreal forest ecosystem. *Boreal Environ. Res.*, 10, 425-436.
- Ruuskanen, T. M., Taipale, R., Rinne, J., Kajos, M. K., Hakola, H., Kulmala, M. (2009) Quantitative long-term measurements of VOC concentrations by PTR-MS: annual cycle at a boreal forest site. *Atmos. Chem. Phys. Discuss.*, 9, 81-134.
- Timmermann, V., Solheim, H., Clarke, N., Aas, W., Andreasen, K. (2013) Skogens helsetilstand i 2012. Resultater fra skogskadeovervåkingen i 2012. Ås, Norsk institutt for skog og landskap (Rapport fra Skog og landskap, 12/2013).
- Tørseth, K., Aas, W., Solberg, S. (2001) Trend in airborne sulphur and nitrogen compounds in Norway during 1985-1996 in relation to air mass origin. *Water Air Soil Pollut.*, 130, 1493-1498.

- Tørseth, K., Aas, W., Breivik, K., Fjæraa, A. M., Fiebig, M., Hjellbrekke, A. G. , Lund Myhre, C., Solberg, S., Yttri, K. E. (2012) Introduction to the European Monitoring and Evaluation Programme (EMEP) and observed atmospheric composition change during 1972–2009. *Atmos. Chem. Phys.*, *12*, 5447-5481.
- Wright, R. F. (2008) The decreasing importance of acidification episodes with recovery from acidification: an analysis of the 30-year record from Birkenes, Norway. *Hydrol. Earth Syst. Sci.*, *12*, 353-362.
- Yttri, K. E., Simpson, D., Nøjgaard, J. K., Kristensen, K., Genberg, J., Stenström, K., Swietlicki, E., Hillamo, R., Aurela, M., Bauer, H., Offenberg, J. H., Jaoui, M., Dye, C., Eckhardt, S., Burkhardt, J. F., Stohl, A., and Glasius, M. (2011) Source apportionment of the summer time carbonaceous aerosol at Nordic rural background sites. *Atmos. Chem. Phys.*, *11*, 13339-13357.

Appendix A

Discussion on local contamination

Human activities at the Birkenes Observatory causing local contamination

The Birkenes II station is frequently serviced by the local station manager and by NILU personnel. Vehicular emissions on site lead to short-term air pollution events herein referred to as local contamination. All activities at the station that potentially cause local contamination are, in principle, registered in the station maintenance log book.

The ion signal at m/z 57.070 showed a distinct increase during such periods noted in the log book. This signal derives from $C_4H_9^+$ ions which are commonly formed in the PTR-ToF-MS instrument upon fragmentation of long-chain hydrocarbons generated from local combustion engine emissions. Figure B1 depicts the time series of the m/z 57.070 signal as measured during the summer 2012 (upper panel) and winter 2013 (lower panel) campaigns, respectively. The mixing ratio should be taken as indicative only since the identity of the neutral precursors is unknown. The green line indicates the time series of data obtained after applying a basic quality-control filter that excludes periods with ion source instabilities and other acquisition software errors (see Methodology section). The blue line was obtained after removing local contamination events as noted in the station log book.

In total, 0.69 % of the 2012 data and 0.98 % of the 2013 data were filtered because affected by local contamination. Figure A1 suggests that the records in the station log book do not capture all local contamination events. The spikes coloured in blue indicate periods potentially affected by local vehicular emissions that have not been registered in the station maintenance log book. These data were, however, not removed from the data that were archived and subjected to further analysis. Any conclusions drawn from data obtained during such periods need to be critically examined for a potential bias by local contamination.

Figure A2 shows a histogram of the duration of local contamination events including the data obtained during 2012 and 2013. Local contamination events typically occur on short time scales (minutes, tens of minutes) confirming the need for highly time resolved measurements of a contamination tracer.

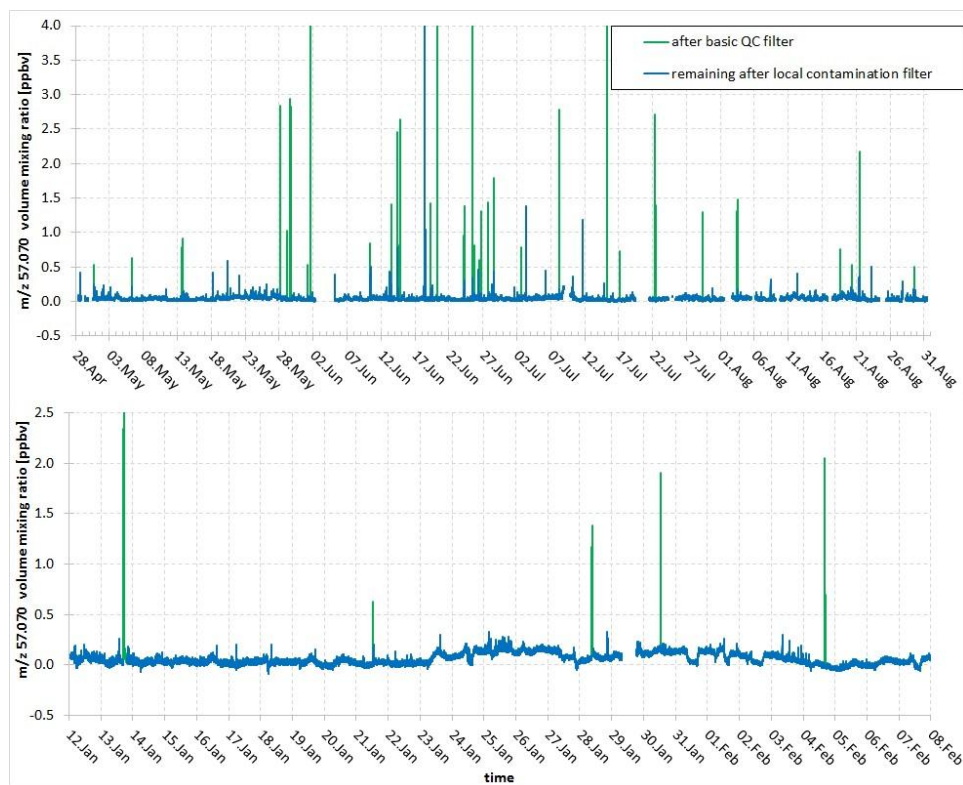


Figure A1: Time series of the m/z 57.070 signal, a vehicular combustion tracer, for the measurement campaigns in 2012 (upper panel) and in 2013 (lower panel). The green line indicates the time series of all data obtained after applying a basic quality-control filter that excludes periods with ion source instabilities and other instrumental deficiencies. The blue line was obtained after removing local contamination events as noted in the station log book. Spikes coloured in blue indicate periods potentially affected by local vehicular emissions that were not registered in the station log book.

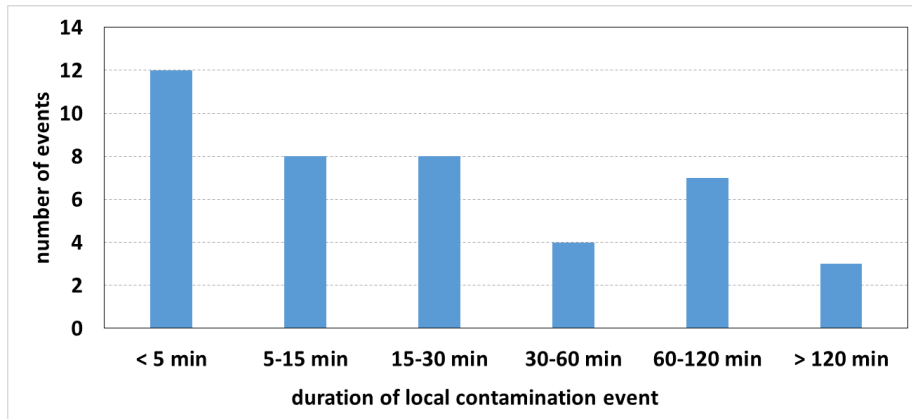


Figure A2: Histogram of the duration of local contamination events including the 2012 and 2013 data. Local contamination events typically occur on short time scales (minutes, tens of minutes) confirming the need for highly time resolved measurements of a contamination tracer



REPORT SERIES SCIENTIFIC REPORT	REPORT NO. OR 1/2014	ISBN: 978-82-425-2637-3 (print) 978-82-425-2638-0 (electronic)	ISSN: 0807-7207
DATE 28.1.2014	SIGN. 	NO. OF PAGES 47	PRICE NOK 150.-
TITLE VOC measurements by PTR-ToF-MS at the Birkenes Observatory A data summary report		PROJECT LEADER Armin Wisthaler	NILU PROJECT NO. N-113006
AUTHOR(S) Stephan Langebner, Tomáš Mikoviny, Markus Müller and Armin Wisthaler		CLASSIFICATION * A	CONTRACT REF.
QUALITY CONTROLLER: Sverre Solberg			
REPORT PREPARED FOR NILU			
ABSTRACT A high resolution proton-transfer-reaction time-of-flight mass spectrometer (PTR-ToF-MS) was used for on-line and real-time measurements of volatile organic compounds (VOCs) at the Birkenes Observatory in Southern Norway. Measurements were carried out during late spring and summer 2012 and in January and early February 2013. Here we present the obtained PTR-MS standard data product which includes volume mixing ratios of methanol, acetonitrile, acetaldehyde, acetone, dimethyl sulphide, isoprene, methacrolein plus methylvinylketone, methylethylketone, benzene, toluene, C8-alkylbenzenes, C9-alkylbenzenes and the sum of the monoterpene isomers. Exploratory data of formic acid, acetic acid, pinonaldehyde and three unidentified signals (m/z 87.080, m/z 89.060 and m/z 101.098) are also shown. PTR-ToF-MS mass spectra were dominated by oxygenated VOCs both in summer and in winter. Pure hydrocarbons were mostly aromatic hydrocarbons (benzene, toluene, C8-alkylbenzenes) in winter and biogenic hydrocarbons (monoterpenes and isoprene) in summer. The summertime data confirm that the Birkenes Observatory is an interesting site in the boreo-nemoral vegetation zone where it is possible to observe both monoterpene and isoprene emissions and their photochemical processing in the atmosphere.			
NORWEGIAN TITLE VOC-målinger med PTR-ToF-MS på Birkenes-observatoriet. En sammendragsrapport			
KEYWORDS Environmental chemistry	Data collection and organisation		
ABSTRACT (in Norwegian) Et høy-oppløselig «proton-transfer-reaction time-of-flight» massespektrometer (PTR-ToF-MS) ble brukt til online, sanntids målinger av flyktige organiske forbindelser (VOC) på Birkenes-observatoriet i Sør-Norge. Målingene ble utført i løpet av våren og sommeren 2012, og i januar og begynnelsen av februar 2013. Her presenterer vi standard dataprodukter fra PTR-MS-målingene, slik som volumblandingsforhold av metanol, acetonitril, acetaldehyd, acetone, dimetylsulfid, isopren, metacrolein + metylvinylketon, metyletylketon, benzen, toluen, C8-alkylbenzener, C9-alkylbenzener og summen av monoterpene-isomerer. Forsøksvise data for maursyre, eddiksyre, pinonaldehyd og tre uidentifiserte signaler (m/z 87.080, m/z 89.060 og m/z 101.098) er også rapportert. PTR-ToF-MS-massespektrene ble dominert av oksygenerte VOCer både om sommeren og vinteren. De rene hydrokarbonene besto for det meste av aromatiske hydrokarboner (benzen, toluen, C8-alkylbenzener) om vinteren og biogene hydrokarboner (monoterpenene og isopren) om sommeren. Sommerdataene bekrefter at Birkenes-observatoriet er et interessant område i den boreo-nemorale vegetasjonssonen hvor det er mulig å observere både utslipp av monoterpenene og isopren og deres fotokjemiske omvandling i atmosfæren.			

* Classification
A Unclassified (can be ordered from NILU)
B Restricted distribution
C Classified (not to be distributed)

REFERENCE: O-113006
DATE: JANUARY 2014
ISBN: 978-82-425-2637-3 (print)
978-82-425-2638-0 (electronic)

NILU – Norwegian Institute for Air Research is an independent, nonprofit institution established in 1969. Through its research NILU increases the understanding of climate change, of the composition of the atmosphere, of air quality and of hazardous substances. Based on its research, NILU markets integrated services and products within analyzing, monitoring and consulting. NILU is concerned with increasing public awareness about climate change and environmental pollution.